The tr ds of the relationships between the concentration (or particle size) and the three quantitative indices are summarized in Table 2. In conclusion, the area-based cr erion F_A is a more sensitive and robust measure of dispersibility than the box- ounting fractal dimension F_C, whereas the degree of mixedness M is unsatisfa ory. In addition, M is not suitable at all when the particle size is tiny compare to the sample area.

5.2. Non- deal dispersion

The purp se here is to find out what happens to the values of F_A and F_C when the number r io of B to A particles is varied to yield a non-ideal dispersion, a hybrid mixture o two different ideal dispersions. The N–U or B–A ratios investigated are summ rized in Table 1. An N–U ratio of 25 means that, of the total number, 25% of t particles (B) is normally dispersed (N) and the rest (A) is uniformly dispersed U). For simplicity, only the percentage of B particles will be specified hencefort Since it has been ascertained above that the particle size does not affect the value of F_A and F_C, the size is fixed at 0.5 units. The relationships between the total c ncentration C and the observed F_A and F_C are depicted in Figs 8 and 9, respectiv y.

From F . 8, it can be seen that except at B = 0% (completely uniform), for every fixed N– ratio, F_A decreases steeply as the total concentration increases. This is becaus F_A is dominated by the normally dispersed B particles whose absolute number i reases. Thus it may be concluded that F_A is a sensitive index of the

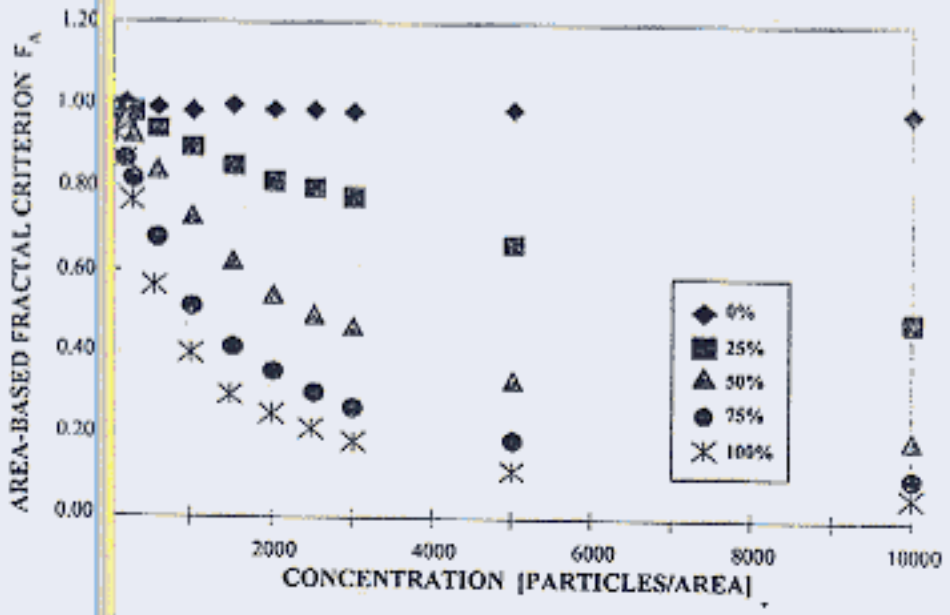

Figure 8. T al concentration versus area-based fractal criterion at each N–U ratio.

n[illegible]-ideality of a dispersion. The higher the total concentration, the more sensitive th[illegible] area-based fractal criterion. Figure 9 reveals that, for every fixed N–U ratio, F_C increases, as the total concentration increases, especially at low concentrations. This is because F_C is dominated by the uniformly dispersed A particles. On the

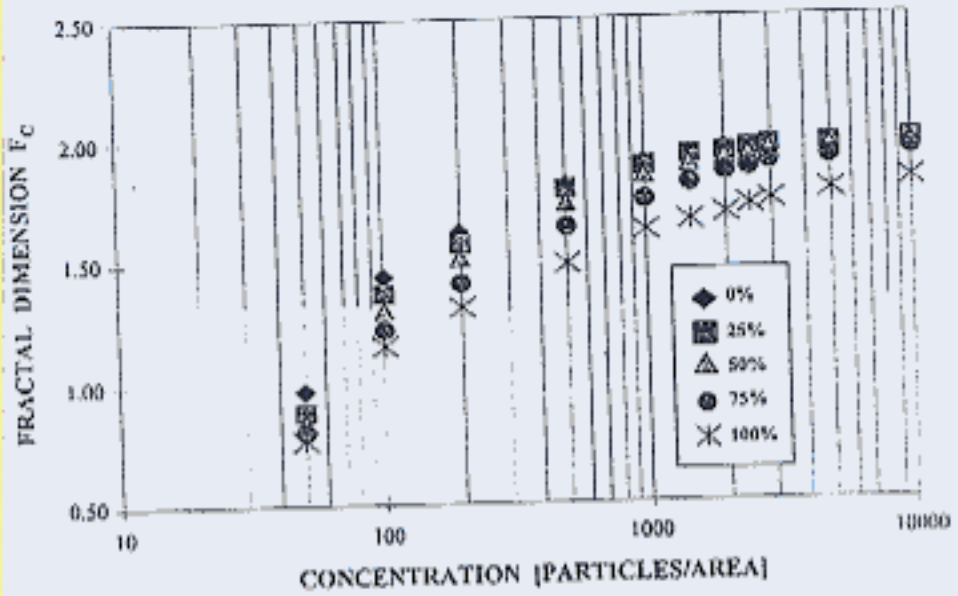

Figure 9. Total concentration versus fractal dimension F_C at each N–U ratio.

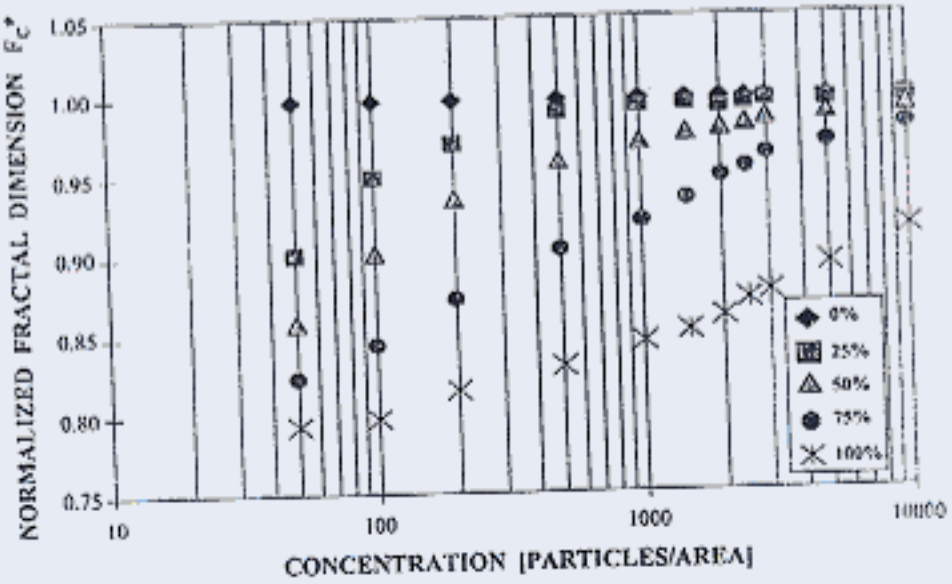

Figure 10. Relationship between the total concentration and normalized fractal dimension at each N–U ratio.

other hand, at a fixed concentration, differences in F_C values among different N–U ratios are less distinct at 0% up to 50%.

Figures 10 shows the relationships between the total concentration versus F_C^* at each N–U ratio. The figure is handy when one wants to interpret an experimentally obtained dispersion pattern in terms of its observed fractal dimension.

6. APPLICATION TO THE INTERPRETATION OF EXPERIMENTAL RESULTS

Phingchin has found experimentally that the kneading temperature is one important factor that affects the dispersion state of pigments in a polymer, i.e. a higher temperature (from 170 to 210°C) leads to improved dispersibility. Table 3 lists the experimental values of F_C^* reported by Phingchin [14].

When the experimental F_C^* at different temperatures are compared, one sees that carbon black kneaded at 210°C was more nearly uniformly dispersed in polystyrene than at 170°C. So was iron oxide. This is because the viscosity of the polymer melt became lower at a higher temperature. When carbon black and iron oxide are compared at the same kneading temperature, one realizes that the former is more uniformly dispersed than the latter because carbon black is organic, non-polar and more compatible with polystyrene. In fact, uniform dispersion is achieved if the normalized fractal dimension is essentially 1. At 170°C kneading temperature, the experimental F_C^* is 0.964. From Fig. 10, at the same 160 total particle concentration, it is found by interpolation that a mixture of identical A and B particles consisting of 28% B (N-type dispersion) and 72% A (U-type dispersion) would have the same fractal dimension of 0.964. In other words, the achieved dispersion is equivalent to one in which 28% of the particles are normally dispersed with the remaining 72% being uniformly dispersed. The equivalent N–U ratios for the other cases are also listed in Table 3.

Similarly, Fig. 8 is a handy tool to interpret the experimental dispersion state from the observed F_N value.

Table 3.
Reported experimental values of the normalized box-counting fractal dimension

Pigment	Kneading temperature (°C)	Speed of screw (r.p.m.)	Feed rate (g/min)	Number of particles counted	Normalized fractal dimension	N–U ratio (normal: uniform) % *N*
Carbon black	170	81	4.5	160	0.964	28
	210	81	4.5	193	0.996	2
Iron oxide	170	81	4.5	88	0.914	50
	210	81	4.5	113	0.935	35

7. CONCLUSIONS

The following conclusions can be drawn:

(1) The degree of mixedness for both the uniform and normal dispersions tends to decrease as the additive concentration or particle size increases.

(2) The area-based fractal criterion and box-counting fractal dimension are more suitable indices than the degree of mixedness because they are not affected by the particle size. The former appears to be a more sensitive index for measuring dispersibility than the latter.

(3) Figures 8 and 10 are handy for evaluating experimentally obtained dispersion pattern. Using the observed value of F_A or F_C^*, they tell us how close the observed dispersion is to the normal dispersion (or to the uniform dispersion) by giving an equivalent percentage of normally dispersed B particles (or uniformly dispersed A particles) in the material matrix.

Acknowledgements

Financial support from National Metal and Materials Technology Center for the research project, financial support from Thailand Research Fund for W. T. and T. C., and academic scholarship from National Science and Technology Development Agency for M. S. are acknowledged.

REFERENCES

1. P. M. C. Lacey, Developments in the theory of particle mixing. *J. Appl. Chem.* **4**, 257–268 (1954).
2. K. Miyanami, in: *Powder Technology Handbook*, K. Iinoya, K. Gotoh and K. Higashitani (Eds), pp. 595–613. Marcel Dekker, New York (1998).
3. B. H. Kay, Specification of ruggedness and/or texture of a line profile by its fractal dimension. *Powder Technol.* **21**, 1–16 (1978).
4. J. C. Graf, The importance of resolution limits to the interpretation of fractal descriptions of fine particles. *Powder Technol.* **67**, 83–85 (1991).
5. N. Yabe, K. Terashita, K. Izumida and K. Miyanami, Dispersion of carbon black in resin by a continuous kneader and its assessment. *J. Soc. Mater. Sci., Japan* **37**, 1344–1348 (1988).
6. Y. Mizuno, K. Terashita and K. Miyanami, Application of fractal dimension for evaluation of dispersion of filler in composite material. *J. Soc. Mater. Sci., Japan* **42**, 836–842 (1993).
7. Y. Mizuno, K. Terashita and K. Miyanami, Evaluation of dispersion state of electrically conductive resin with fractal dimension. *Kagaku Kogaku Ronbunshu* **19**, 21–29 (1993).
8. Y. Mizuno, K. Terashita and K. Miyanami, Operating plan for continuous kneading of electrically conductive resin with analysis of time series. *Kagaku Kogaku Ronbunshu* **19**, 13–20 (1993).
9. K. Terashita, T. Tanaka and K. Miyanami, Continuous kneading for electrically conductive composite material and evaluation of filler dispersion state. *Bull. Univ. Osaka Pref.* **42**, 1–17 (1993).
10. K. Terashita, T. Teshima, N. Yabe and K. Miyanami, The mixing of toner composition and its evaluation. *J. Soc. Powder Technol., Japan* **30**, 556–562 (1993).

11 W. Tanthapanichakoon, T. Charinpanitkul and P. In-eure, Application of novel concept of fractal to study dispersion of additive in plastic, in: *Proc. Ann. Meeting of The Engineering Institute of Thailand*, Bangkok, Thailand (1995).
12 W. Tanthapanichakoon, T. Charinpanitkul and P. In-eure, Experiment on compounding polyethylene resin with iron oxide pigment using twin-screw kneaders, in: *Proc. 1995 Regional Symp. on Chemical Engineering*, Bangkok, Thailand (1995).
1. P. In-eure, Effect of kneading conditions on the dispersion of pigments in polyethylene using a continuous kneader, Master's thesis, Chulalongkorn University, Bangkok, Thailand (1994).
1- N. Phingchin, Factors influencing the dispersion of pigments in polystyrene upon using a continuous twin-screw kneader, Master's thesis, Chulalongkorn University, Bangkok, Thailand (1996).
1 A. Thongchiew, Factors influencing the dispersion of organic pigments in polyethylene upon using a continuous twin-screw kneader, Master's thesis, Chulalongkorn University, Bangkok, Thailand (1997).
1 M. Suphawita, Development of quantitative indices for evaluating the degree of dispersion of additives in compounded material using computer experiments, Master's thesis, Chulalongkorn University, Bangkok, Thailand (1997).
W. Tanthapanichakoon, Stochastic analysis of a high-rate activated sludge wastewater treatment plant with random diurnal plant inputs and random process parameters, via Monte-Carlo simulation, Doctoral dissertation, University of Texas at Austin (1978).
T. Yano and Y. Sano, *J. Soc. Chem. Eng., Japan* 29, 214 (1965).
A. Tsuchinari, Y. Hokii, S. Osamu and C. Kanaoka, Effects of Al_2O_3–TiO_3 contents on structure and permeability of porous magnesia ceramic — fractal of pore characteristics, *J. Ceramic Technol., Japan* 99, 561–566 (1991).

ELSEVIER

Powder Technology 118 (2001) 97–106

POWDER TECHNOLOGY

www.elsevier.com/locate/powtec

Stochastic simulation of the agglomerative deposition process of aerosol particles on an electret fiber

C. Kanaoka [a,*], S. Hiragi [a], W. Tanthapanichakoon [b]

[a] Department of Civil Engineering, Faculty of Engineering, Kanazawa University, 2-40-20 Kodatsuno, Kanazawa 920-8667, Japan
[b] Faculty of Engineering, Chulalongkorn University, Pathumwan, Bangkok 10330, Thailand

Abstract

To design a high-performance air filter with a longer service life, we need to predict how the morphology of particle accumulates on a constituent fiber changes and affects the collection efficiency and pressure drop of the filter under dust-loaded condition. This paper describes a practical three-dimensional simulation method for predicting the agglomerative deposition process of fine aerosol particles on an electret fiber. The simulated results are shown to agree quite well with the experimental observations for both uncharged and charged particles. For the former, only the gradient force, and for the latter, the coulombic force needs to be considered as long as an oncoming particle has not come in close proximity to any previously deposited particles. In contrast, once the oncoming particle enters a region of close proximity to a deposited particle at the tip of a dendrite or chain-like agglomerate, it suffices to consider only the high-gradient or particle string formative force in the present stochastic model. © 2001 Elsevier Science B.V. All rights reserved.

Keywords: Electret filtration; Dendrites; Agglomerates; Electrostatic effect; Dust load

1. Introduction

An electret fiber is made of permanently polarized dielectric material. Compared to a similar nonpolarized fiber, the aerosol collection efficiency of the electret fiber can be significantly higher, even if the aerosol particles are uncharged. Thus, electret fibers have been used to enhance the collection efficiency of HEPA and ULPA filters. In some instances, the collection efficiency of an electret fiber may drop substantially as deposition of the particles progresses. Typically, air filters are not equipped with any dust-cleaning systems and is discarded when captured particles clog the air passage. Kanaoka [1] showed how to double the service life by designing a filter with larger dust-holding capacity at the same final pressure drop for the filter composing of uncharged fibers (uncharged filter). This is achievable because filter performance depends not only on filtration conditions and particle properties but also on filter properties, such as fiber diameter, packing density, and packing structure.

As more and more particles deposit on a fiber inside a filter and/or on previously captured particles, they form complicated accumulates. For uncharged filter, collection efficiency increases as particles deposit. However, for the case of electret filter, it is experimentally known to decrease with particle collection in the initial stage of the collection. The accumulation process of this has not been simulated previously and if it is needed to design a filter with improved service life, we need to predict filter performance under dust load, which requires good understanding of how the morphology of particle accumulates on a fiber affects the collection efficiency and pressure drop of a dust-loaded filter [1].

1.1. Experimental observation of deposition pattern on a single fiber

Figs. 1 and 2 show how the agglomerates of uncharged and charged particles, respectively, change with filtration time and location on an electret fiber. When uncharged particles are collected, they attach all around the fiber and form chain-like agglomerates, which subsequently become irregular and complicated as the electrostatic effect gradually weakens. In the case of charged particles, the shape is

* Corresponding author. Fax: +81-76-234-4645.
E-mail address: kanaoka@t.kanazawa-u.ac.jp (C. Kanaoka).

PII: S0032-5910(01)00299-6

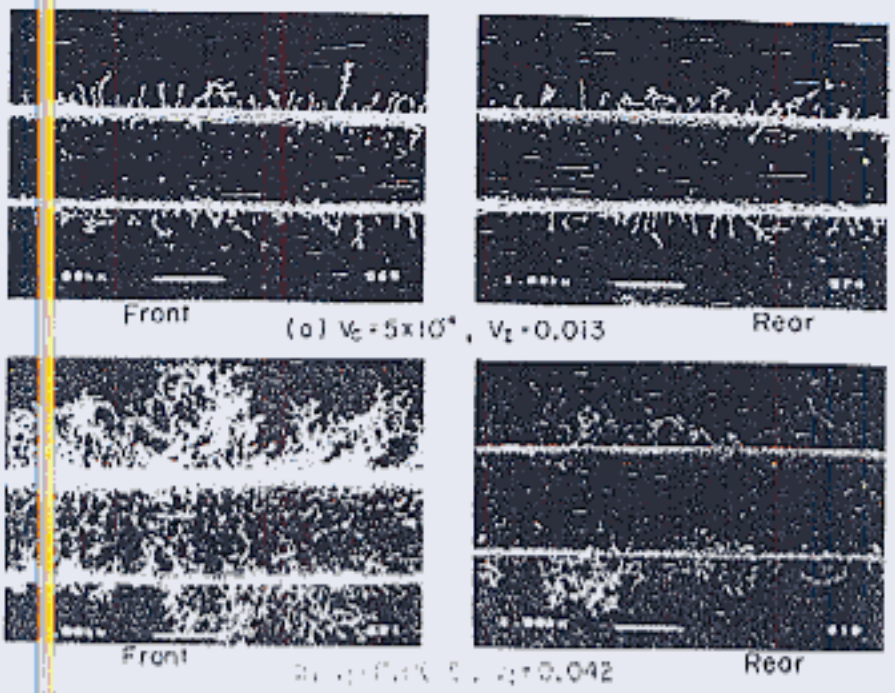

Fig. 1. Experimental deposition of noncharged particles on an electret fiber ($d_f = 30$ μm, $d_p = 0.39$ μm, $u = 15$ cm/s, $\rho_p = 2330$ kg/m^3, $K_{ta} = 0.004$, $Stk = 0.015$, $Pe = 5 \times 10^4$, $R = 0.013$).

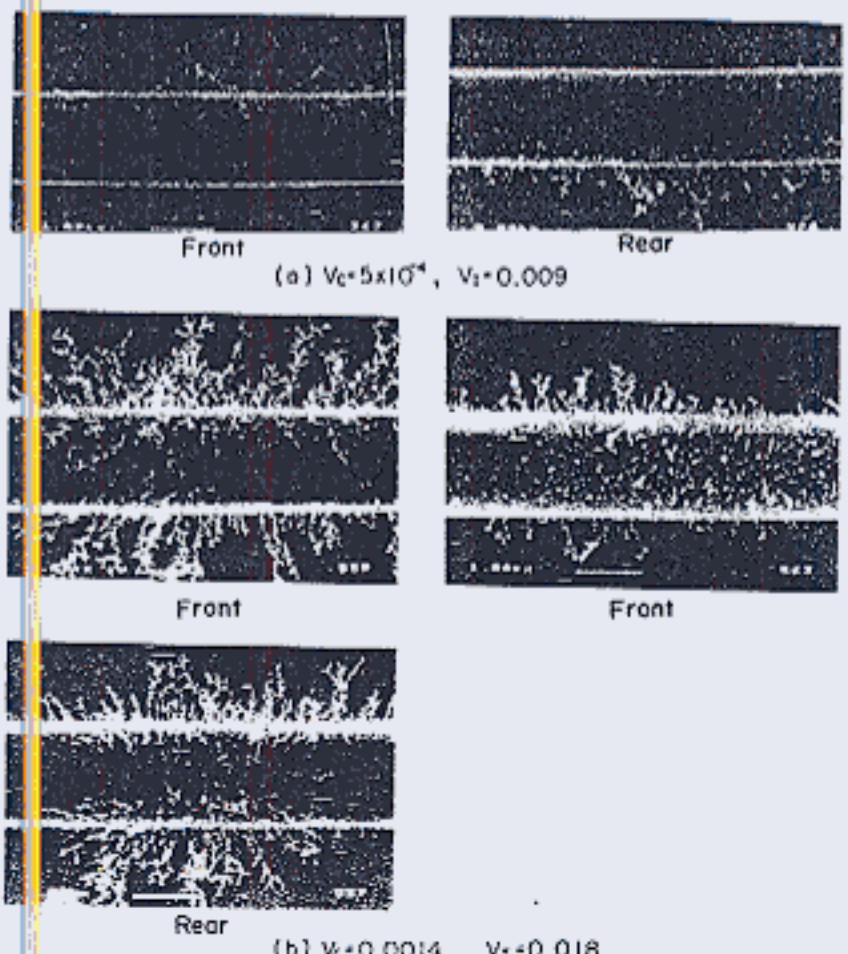

Fig. 2. Experimental deposition of charged particles on an electret fiber ($d_f = 30$ μm, $d_p = 0.39$ μm, $u = 15$ cm/s, $\rho_p = 2330$ kg/m^3, $K_{ta} = 0.004$, $Stk = 0.015$, $Pe = 5 \times 10^4$, $R = 0.013$).

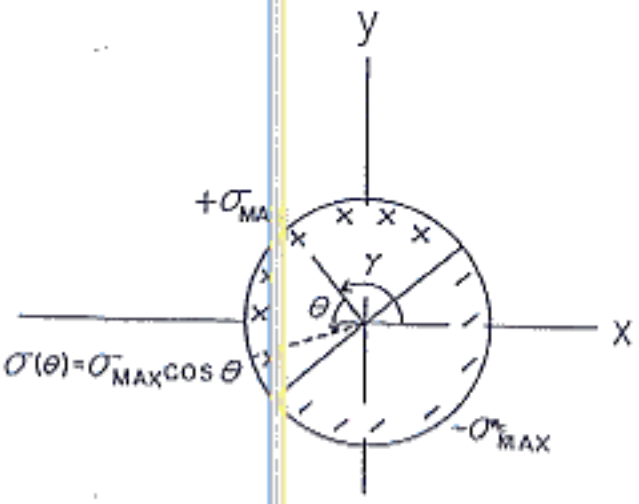

Fig. 3. Charged distribution on the surface of an ideal electret fiber.

similar to the former but agglomerates concentrate in a limited area of opposite polarity to the particles and grows along the electric force line.

1.2. Simulation of deposition process on a fiber

To rigorously simulate the deposition process, we need to calculate the flow field around a dust-loaded fiber that theoretically changes with every deposition of a new particle. Since the process is random, the repetitive recalculation of flow field around such an evolving irregular fiber is prohibitively time-consuming. There are two main approaches to simulate the particle agglomerates on a fiber, namely, the deterministic model [2–4] and the stochastic model [5–17]. The former is capable of describing the average growth of dendrites but does not express the random nature. In contrast, the latter can handle any random process but may take a long time to get meaningful results. Most previous simulations focus on the early stage of collection when the dust load is light and the so-called dendrites are relatively small agglomerates.

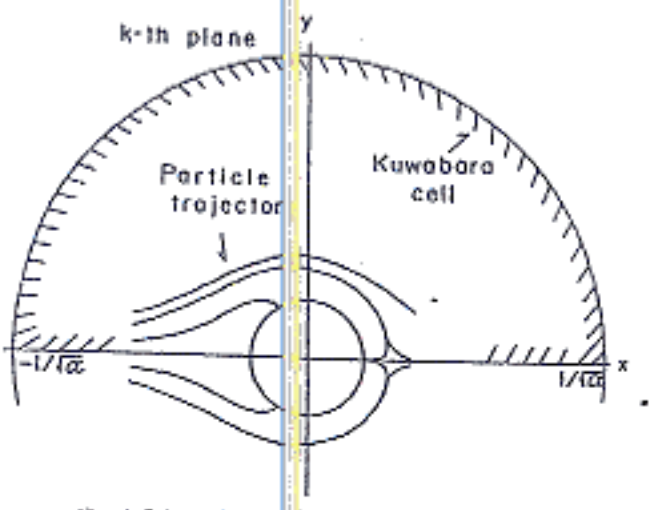

Fig. 4. Schematic of the simulation region ($\beta = 0°$).

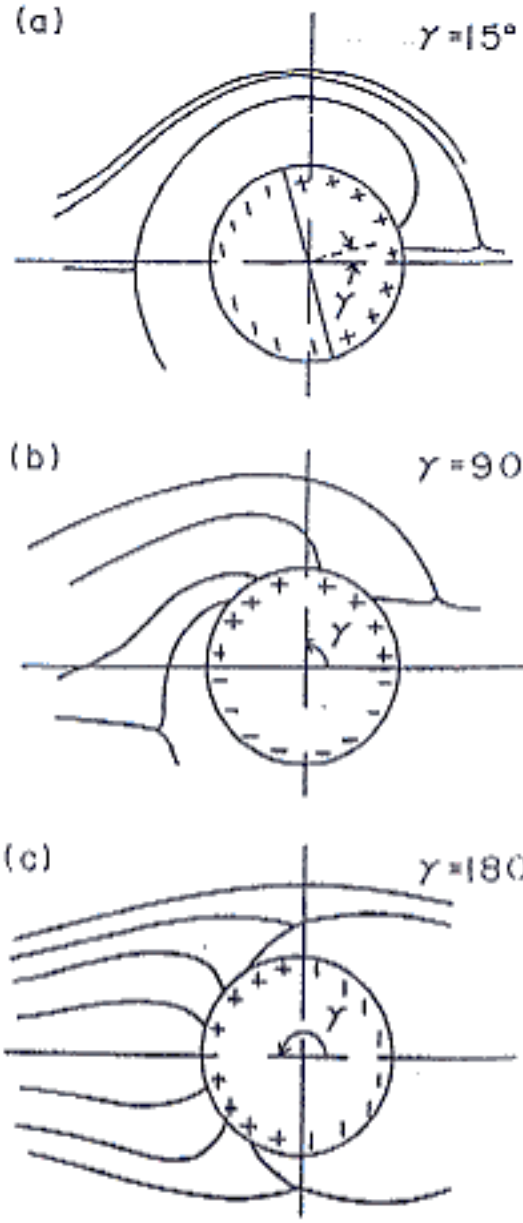

Fig. 5. Variation in the particle trajectories with γ.

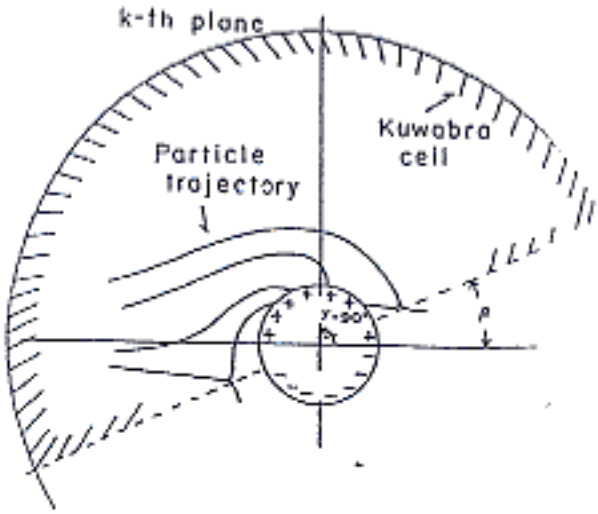

Fig. 6. Schematic of the simulation region ($\beta > 0°$).

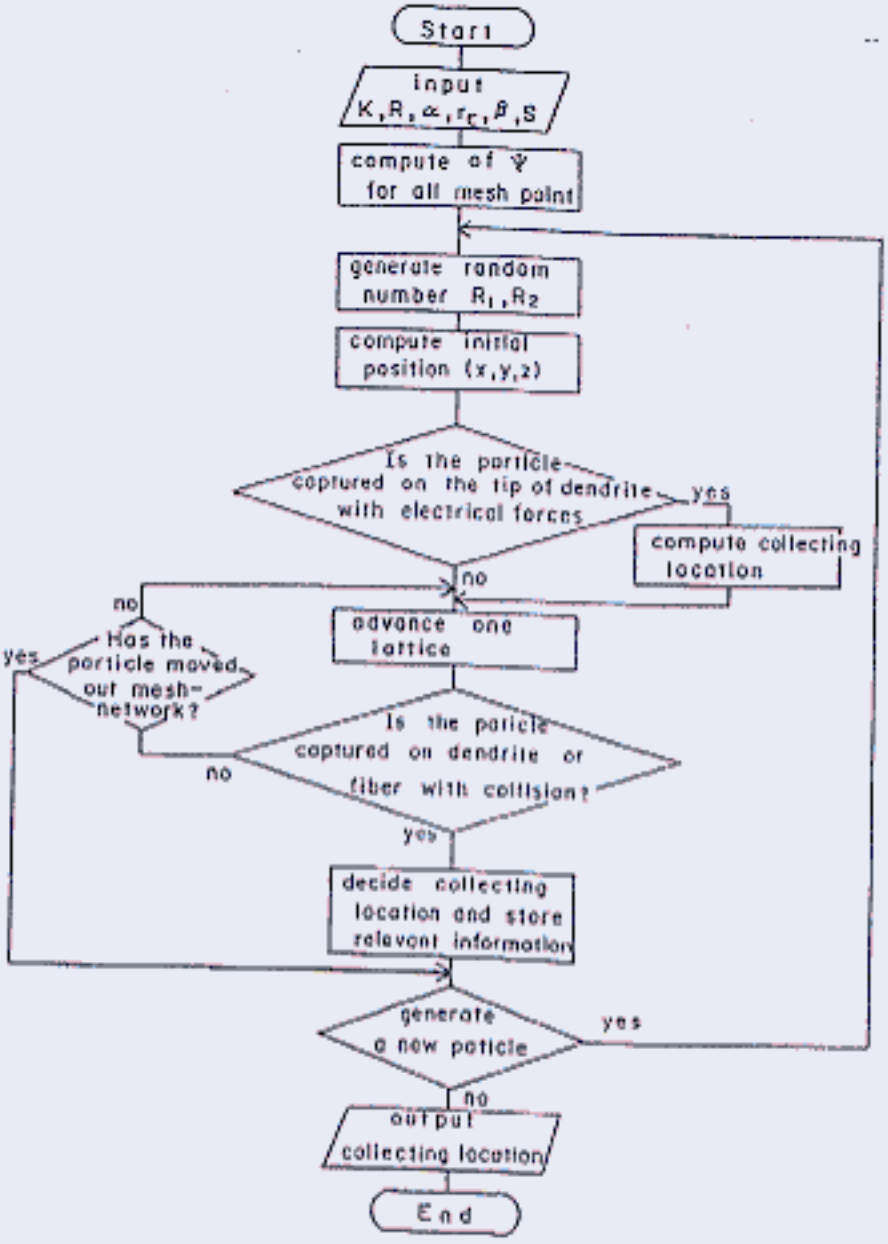

Fig. 7. Simplified flowchart of the simulation.

The present paper extends our stochastic model to cover the intermediate stage of collection on an electret fiber. What follows is a description of the agglomerative deposition model, presentation and discussion of the simulation results, and conclusion.

2. Stochastic model of deposition process on an electret fiber

Referring to an earlier stochastic mechanical collection model of Kanaoka et al. [7], Baumgartner and Loeffler [18] carried out two-dimensional simulation of particle deposition on an electret fiber. Since a three-dimensional model more closely represents the actual process and reveals additional morphological details, it is adopted in the present work.

2.1. Electrostatic forces acting on a particle near an electret fiber

Coulombic forces, F_C (between the particle and fiber) and F_{CP} (between the particle and another nearby particle), and image force, F_I, come into play only when a particle

Table 1
Simulation conditions

Electrical parameters	K_C, K_{I_0} [–]	0.1, 1.0
Interception parameter	R [–]	0.05
Filter packing density	α [–]	0.06
Fiber diameter	d_f [–]	2.0
Height of generation in y-direction	H [–]	3.0
Mesh number in z-direction	S [–]	50

has electric charge. For both charged and uncharged dielectric particles, the long-range nonuniform electric field around the electret fiber and the agglomerates lead, respectively, to the long-range gradient force, F_G, and particle string formative or high-gradient force, F_R. Under typical filtration conditions Hiragi [19] has calculated that F_R becomes dominant when an oncoming particle comes in close proximity to a deposited particle and that, until this proximity region is reached, only either F_C, in the case of charged particles, or F_G, in the case of uncharged particles, need to be considered. His conclusions agree with Zebel [20] and are adopted here.

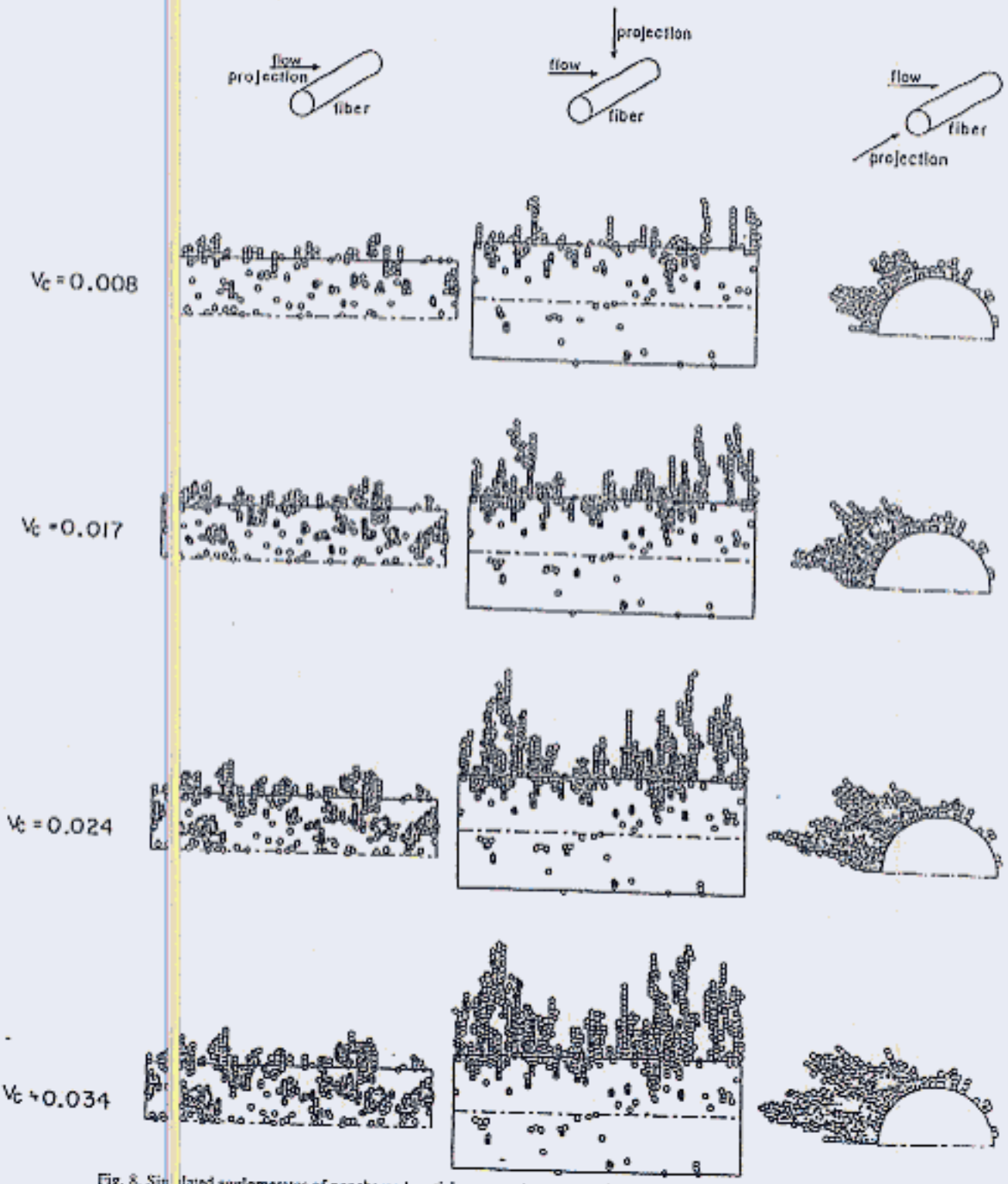

Fig. 8. Simulated agglomerates of noncharged particles on an electret fiber ($K_h = 0.1$, $R = 0.05$, $\alpha = 0.06$, $r_f = 2d_p$).

2.2. Region of simulation

Fig. 3 shows the ideal distribution of charges on the electret fiber surface. It is assumed that the surface charges will not decay as particles deposit on the fiber. The flow of fluid around the fiber is Kuwabara flow [21].

2.2.1. Uncharged particles

As explained before, the trajectory of an oncoming uncharged particle is essentially determined by the gradient force, F_G, except in a region of close proximity to a deposited particle. Since F_G depends only on the radial coordinate r and not on the polarization direction γ, the simulation region shown in Fig. 4 is general and convenient to use.

2.2.2. Charged particles

For charged particles, the coulombic force, F_C, essentially determines the trajectory, except in the region of

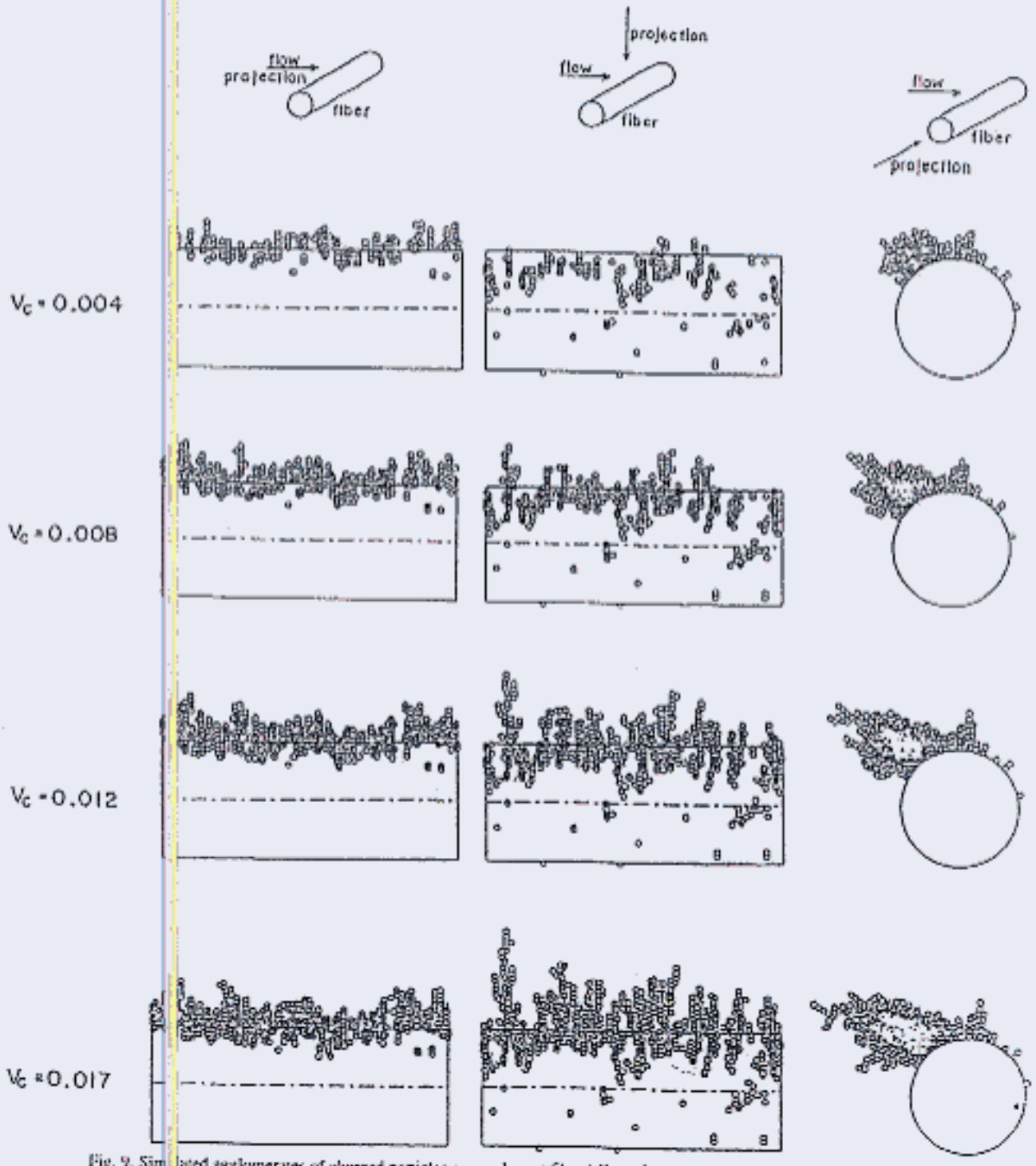

Fig. 9. Simulated agglomerates of charged particles on an electret fiber ($K_C = 0.1$, $R = 0.05$, $\alpha = 0.06$, $\gamma = 0°$, $r_c = 2d_p$).

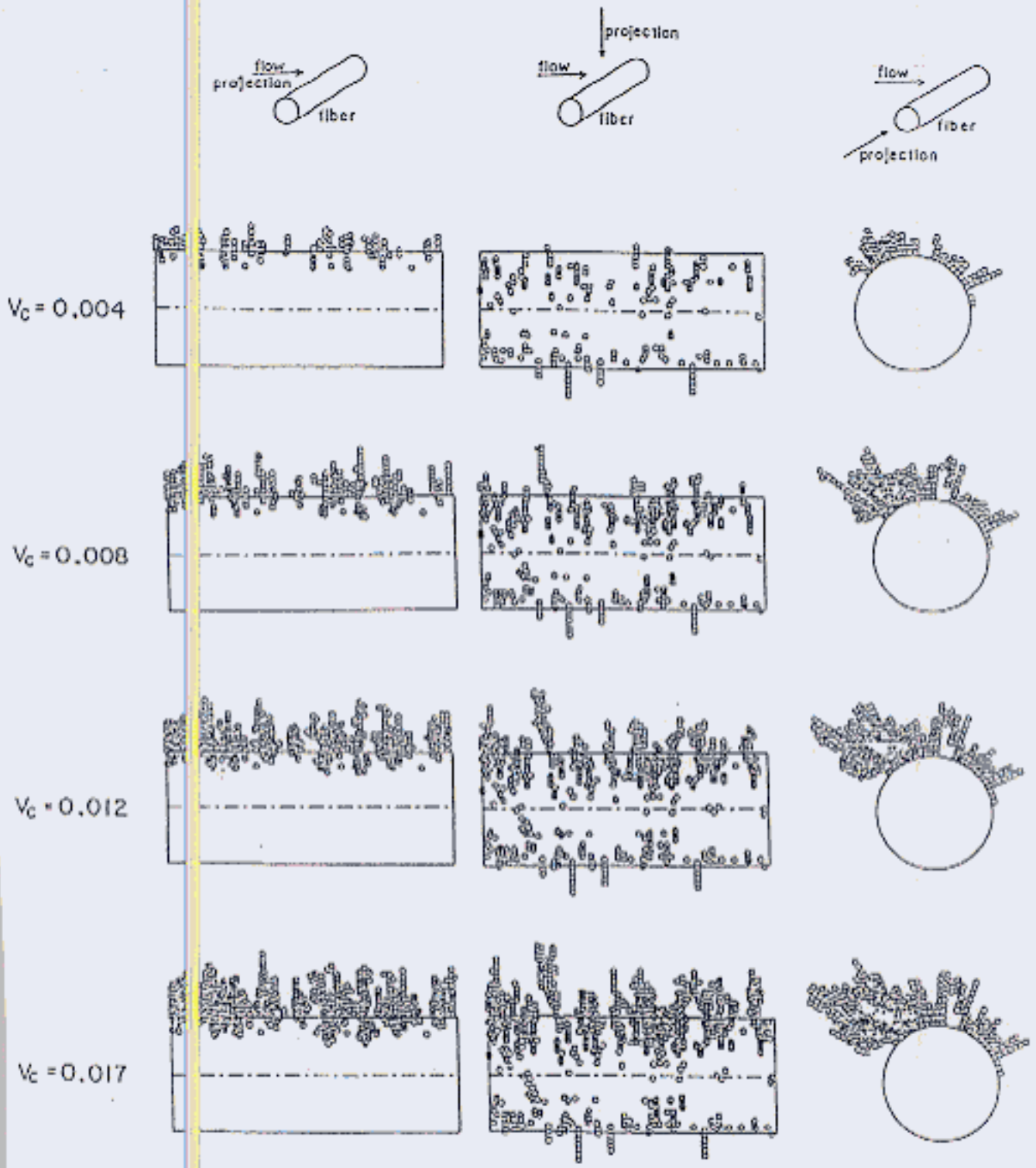

Fig. 10. Simulated agglomerates of charged particles on an electret fiber (K_c = 1.0, R = 0.05, α = 0.06, γ = 0°, $r_c = 2d_p$).

lose proximity to so e deposited particle. Since F_c de- ends on the polari tion direction γ as well as the oordinates r and θ. e resulting trajectory changes dras- ically with γ. Fig. illustrates the effect of γ on the rajectories. In this c e, the simulation region is as de- icted in Fig. 6, nam y, the hatched half of an imaginary ylindrical cell obtai d by a plane passing through the wo critical points on e limiting trajectories.

2.3. Calculation of trajectories and Monte-Carlo simulation of deposition process

The trajectory of an oncoming particle around an electret fiber outside the region of proximity to deposited particles may be expressed by either Eq. (1) or (2).

Uncharged particle: $V - U = K_h F_G$ (1)

Charged particles: $V - U = K_c F_c$ (2)

To reduce the simulation time, an imaginary mesh network is constructed around the fiber and the corresponding heights on the particle generation plane for the trajectories passing through all the lattice points are deter-

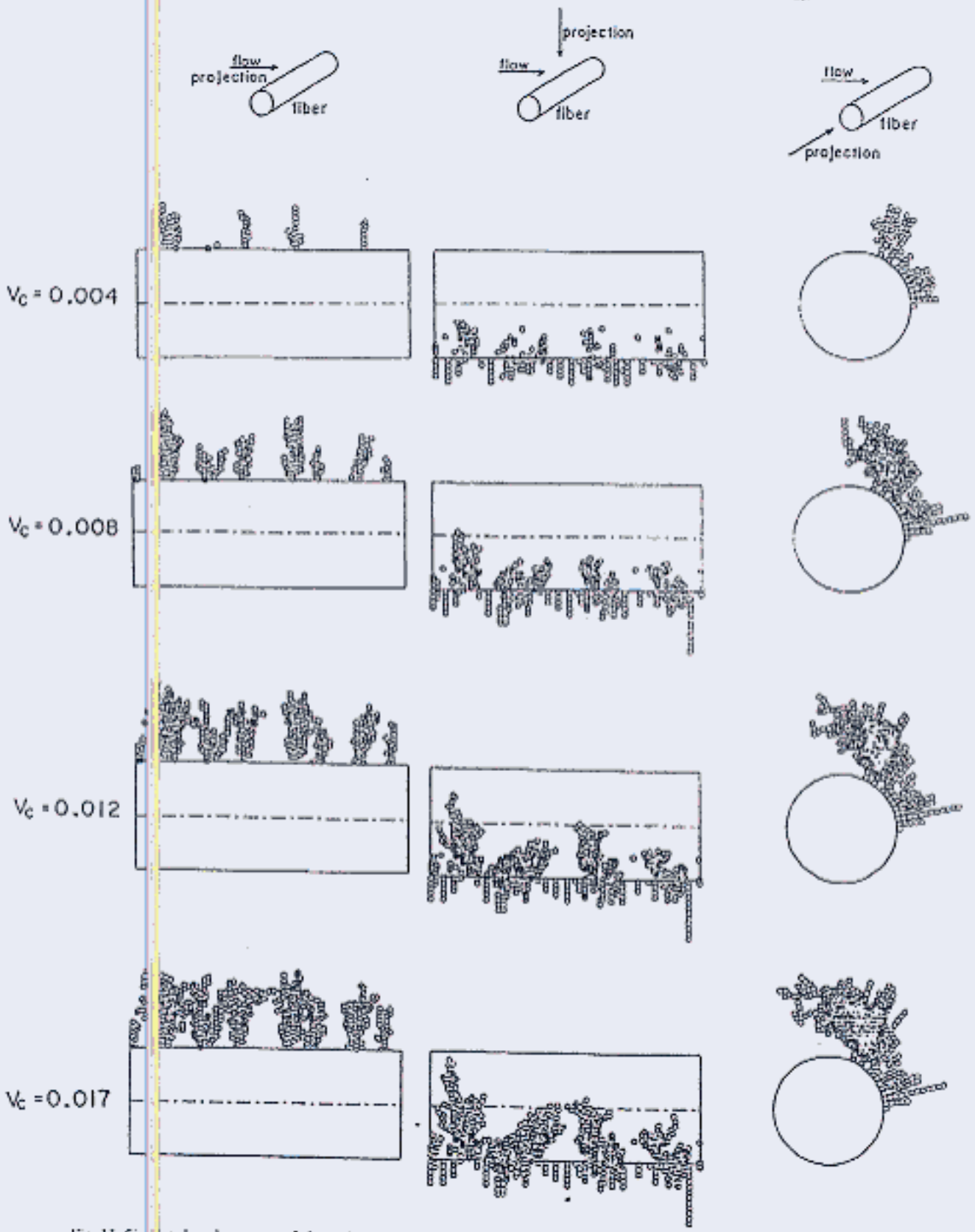

Fig. 11. Simulated agglomerates of charged particles on an electret fiber ($K_c = 1.0$, $R = 0.05$, $\alpha = 0.06$, $\gamma = -45°$, $r_f = 2d_p$).

mined at the start of each simulation. These values are handy for subsequen step-by-step determination of the trajectory of an oncor ing particle [7].

As an oncoming p ticle comes in close proximity to a deposited particle, its novement is controlled by the high-gradient force, F_R. A cording to the calculation result of Zebel [20], the high-g adient electrostatic field is promi-nent only at the tip o the particle string (dendrite). Thus, only the electrostatic f eld around the dendrite tip needs to be considered. Once a oncoming particle enters this pro-jected hemisphere of i fluence of the high-gradient field at the dendrite tip, it is as umed to deposit at the center of the hemisphere [19].

2.4. Flowchart and co dition of simulation

Fig. 7 presents a si plified flowchart of the simulation algorithm. To accoun for the effect of the high-gradient force, F_R, at the tip of a candidate dendrite, a newly generated particle is fi t checked to see whether its traje-tory passes inside the h misphere of influence described in Section 2.3. If it doe , then the location of capture is calculated and kept as candidate. Next, the same particle is allowed to move inc mentally while checking is carried out at each step to se whether it collides with the fiber surface or one of the eposited particles. If it does, then the location of collisio is compared with the first candi-date and the one furth from the fiber surface is selected. If no collision occurs, t en the first candidate is selected. If there is no candidate, hen the particle is not captured. Table 1 lists the variou simulation conditions investigated.

3. Simulation results a d discussion

Figs. 8 and 9 shov the time dependence of particle agglomerates simulated or the case of uncharged particles ($K_{In} = 0.1$) and charge particles ($K_C = 0.1$), respectively. Evidently, the chain-li structures of particle agglomer-ates are similar to the perimental observation shown in Figs. 1 and 2. In all mulations, the radius r_E of the hemisphere of influenc is taken to be $2d_p$ because this euristic value has bee found in a preliminary study to give results most resem ing the experimental observations 19]. Comparison betwe n Figs. 8 and 9 at the same dust oad V_c reveals that ch ged particles tend to form taller dendrites that concentra e on a more limited area on the fiber surface than the ase of uncharged particles. This tendency is also observe experimentally. Because of space limitation, only two mo simulation results are shown in Fig. 10 ($K_C = 1$; $\gamma = 0°$ and Fig. 11 ($K_C = 1$; $\gamma = -45°$). Comparison between F s. 9 and 10 reveals that, at the same dust load, more p ticles deposit on the rear surface as the coulombic force F_R, is much stronger than the gradient force, F_G. Of c rse, the collection efficiency also increases appreciably. C mparison between Figs. 10 and 11 clearly confirms the strong effect of the polarization direction γ on the spatial distribution of particles on the fiber surface. The effect of γ on the average shape of dendrites is hard to elucidate because it is necessary to fully understand how the electrical charges on the deposited particles are transferred among themselves and between them and the electret fiber. In addition, the simulation assumes monodisperse particles and identical charges on all particles. Nevertheless, the present three-dimensional simulation method gives more realistic representation of the particle string structures than Baumgartner and Loeffler [18].

4. Conclusion

The present paper describes a practical method to carry out three-dimensional simulation of the agglomerative deposition process on an electret fiber. The method yields results that agree quite well with the experimental observations. The next study will determine the value of the efficiency-raising factor for the electret fiber under various operating conditions, which would be handy for the prediction of filter performance under dust loads.

Nomenclature

C_m	Cunningham's correction factor
D_{BM}	Brownian diffusion constant
d	fiber or particle diameter
F_C	dimensionless coulombic force
F_G	dimensionless gradient force
F_R	dimensionless high-gradient force
K_C	dimensionless electrical parameter ($= C_m n_p e \bar{\sigma} / 6\varepsilon_0(1+\varepsilon_f)\mu d_p u$)
K_{In}	dimensionless electrical parameter ($= C_m \pi^2(\varepsilon_p - 1)\bar{\sigma}^2 d_p^2 / 6\varepsilon_0(\varepsilon_p + 2)(\varepsilon_f + 1)^2 \mu d_f u$)
m	mass of particles accumulated particles on a fiber
Pe	Peclet number ($= d_f u_0 / D_{BM}$)
r_E	radius of hemisphere of influence of the high-gradient field
R	interception parameter ($= d_p / d_f$)
S	Mesh number in z-direction
s	time
Stk	Stokes number ($= C_m \rho_p d_p^2 u_0 / 9\mu d_f$)
U	dimensionless gas velocity ($= u/u_0$)
u	gas velocity
V	dimensionless particle velocity ($= v/u_0$)
v	particle velocity
V_c	dimensionless volume of accumulated particles on a fiber ($= m\rho_p \alpha$)
α	packing density of fiber
β	direction of simulation region
γ	direction of polarization on an electret fiber
μ	gas viscosity
ρ	air or particle density
Ψ	stream function

Subscript

f	fluid or fiber
p	particle
0	initial

Acknowledgements

W.T. receives financial support from Thailand Research Fund.

References

[1] C. Kanaoka, Performance of an air filter at dust-loaded condition, in: K.R. Spurny (Ed.), Advances in Aerosol Filtration, Lewis Publishers, Boca Raton, 1998, pp. 323–334.
[2] A.C. Payatakes, Filtr. Sep. 13 (1976) 602.
[3] A.C. Payatakes, AIChE J. 23 (1977) 192.
[4] A.C. Payatakes, Grad., AIChE J. 26 (1980) 443.
[5] D.T. Bahrot, C. Tien, S. Wang, AIChE J. 26 (1980) 289.
[6] C. Kanaoka, H. Emi, T. Myojo, Kagaku Kogaku Ronbunshu 5 (1978) 535.
[7] C. Kanaoka, H. Emi, T. Myojo, J. Aerosol Sci. 11 (1980) 377.
[8] C. Kanaoka, H. Emi, W. Tanthapanichakoon, AIChE J. 29 (1983) 865.
[9] C. Kanaoka, H. Emi, S. Hiragi, Proc. 2nd Int. Aerosol Conf., Berlin 1 (1986) 674.
[10] C. Kanaoka, H. Emi, S. Hiragi, T. Myojo, Soc. Powder Technol. Jpn. 24 (1987) 74.
[11] C. Kanaoka, S. Hiragi, K. Yamada, Kagaku Kogaku Ronbunshu 16 (1990) 252.
[12] C. Kanaoka, S. Hiragi, J. Aerosol Sci. 21 (1990) 127.
[13] C. Kanaoka, S. Hiragi, Proc. 12th Int. Symp. Contam. Control 1 (1994) 59.
[14] T. Myojo, C. Kanaoka, H. Emi, J. Aerosol Sci. 15 (1984) 483.
[15] W. Tanthapanichakoon, C. Kanaoka, Proc. 6th World Filtr. Cong. 1 (1993) 514.
[16] S. Wang, M. Beizaie, C. Tien, AIChE J. 23 (1977) 879.
[17] M. Wongsri, W. Tanthapanichakoon, C. Kanaoka, Adv. Powder Technol. 2 (1991) 11.
[18] H. Baumgartner, F. Loeffler, J. Aerosol Sci. 17 (1986) 438.
[19] S. Hiragi, Doctoral dissertation, Kanazawa University, 1995.
[20] G. Zebel, Staub 23 (5) (1963) 263.
[21] S. Kuwahara, J. Phys. Soc. Jpn. 14 (4) (1959) 527.

Journal of Multidisciplinary Research Vol.34 No.1 Spring 2009

学際研究

日本学際会議学会誌

通巻 NO.53

日本学際会議

MULTIDISCIPLINARY RESEARCH COUNCIL OF JAPAN

学際研究

Journal of Multidisciplinary Research

Vol.14 No. 1 (通巻53号)

目 次

国際報文

Development of Odor Control Technology for Crematory Furnace Using Corona Discharge Reaction

Wiwut Tanthapanichakoon*1, Nantamas Dhattavorn*2, Sahat Chaiyo*3
Department of Chemical Engineering, Chulalongkorn University, Thailand
Hajime Tamon*4
Department of Chemical Engineering, Kyoto University, Japan
Noriaki Sano*5
Department of Chemical Engineering, Himeji Institute of Technology, Japan

This article investigates the feasibility of purifying the exhaust gas from cremation using corona discharge reactor with electron attachment effect. Firstly, in a survey of the common gas species emitted from the cremation, it was found that extremely low concentrations of some organic compounds can still cause malodorous smell. Next, the article summarizes the experimental results on removal of sulfur compounds, nitrogen compounds, and organic compounds, including NOx, SOx, and some other malodorous gases from nitrogen or air using corona discharge reactors. In this summary, the influence of coexisting oxygen and water vapor in the treated gas is discussed, indicating that the presence of oxygen and water vapor in the gas contributes to the increase of the removal efficiency in many cases. As for the influence of temperature on treating exhaust gas from incineration such as cremation, temperature elevation negatively affects the removal of SO_2. Furthermore, the reactor structure in terms of the shapes of cathode and anode are discussed.

Introduction

One of the national air pollution problems in Thailand is emission gas from the crematoria during cremation rites. There are nearly 23,000 temples nationwide, including approximately 300 temples with crematory furnaces in Bangkok Metropolitan Area. Various malodorous gases and particulate are emitted during cremation, causing frequent complaints from vicinal communities. Table 1 lists the commonly reported components in crematory emission. Typically crematory gases are emitted from a stack to the atmosphere without adequate treatment. A few rich temples have installed furnaces with after-burning systems but an overwhelming majority of Bangkok temples have inadequate systems, not to mention those in the country side.

Table 2 compares the generic technologies with corona discharge technology for odor control. Under suitable conditions, corona discharge is a novel efficient method that can simultaneously remove several gases. As an important character of the corona discharge, a sufficient number of low energy electrons are produced in gas stream easily. When discharged electrons collide with malodorous gas molecules, some electrons are captured by the gas molecules to form negative ions, which can be separated from the main gas stream in an electric field as solid deposit on the anode surface. First proposed for gas purification by Tamon et al.[4], this phenomenon of "electron attachment" depends on the electron energy, the

*1. Dr. Wiwut Tanthapanichakoon (born in 1949)
Professor, Department of Chemical Engineering and Thai Powder Technology Center, Faculty of Engineering, Chulalongkorn University, Thailand. Ph. D. in University of Texas at Austin.
*2. Nantamas Dhattavorn (born in 1975)
Master Student, Department of Chemical Engineering, Faculty of Engineering, Chulalongkorn University.
*3. Sahat Chaiyo (born in 1978)
Master Student, Department of Chemical Engineering, Faculty of Engineering, Chulalongkorn University.
*4. Dr. Hajime Tamon (born in 1952)
Professor, Department of Chemical Engineering, Kyoto University, Japan. Ph. D. in Kyoto Universitiy.
*5. Dr. Noriaki Sano (born in 1967)
Reseach Associate, Department of Chemical Engineering, Himeji Institute of Technology, Japan. Ph. D. in Kyoto University.

Table Types and concentrations of gaseous emission from a crematorium after 100-fold dilution[15,17,18]

		Components	Concentration	
	Air	N_2	78	%
		O_2	20~21	%
	Low Concentration	CO_2	0.01-0.02	%
		H_2O	0.22	%
		NO_x	80	ppm (max)
		SO_x	5.8	ppm (max)
		Acetic acid (CH_3COOH)	24	ppm
		Hydrocarbons	230	ppm (as propane)
	Very ute concentration (malodorous)	Acetaldehyde	0.04	ppm
		Styrene	0.01	ppm
		Hydrogen sulfide	0.01	ppm
		Methyl mercaptan	0.01	ppm
		Dimethyl sulfide	0.001	ppm
		Ammonia	0.0005	ppm
		Trimethyl amine	0.023	ppm

structure of the g molecules and its electron affinity [15,16,19]. It can lead very high selectivity in the formation of negative ions fr m electronegative impurities even at low concentrations. Under suitable conditions clusters of ions with gas mo ecules are formed, which greatly enhance the remo l efficiency. In the presence of O_2, oxygen radicals an ozone are formed and contribute to decomposition an oxidation of the malodorous gas molecules.

Principle of gas urification

Figure 1 illustrat the principle of gas purification. An impurity AB is to e removed from an inert gas in a cylindrical corona d scharge reactor. Its cathode is a wire tightened at the cen r of the reactor and the stainless steel cylinder is the ano e. High DC voltage (-5~-15 kV) is applied to the cathe e to induce corona discharge in the reactor. During thei drift to the anode, electrons emitted by the discharge collide with some of the gas molecules and the resulting negative ions drift to and deposit on the anode. The present paper describes the joint development of the corona discharge reactor by Tamon et al., Sano et al. and Tanthapanichakoon et al. to control malodorous crematory emission.

Experimental Setup

As illustrated in Figure 2, the experimental set-up and experimental procedure have been reported elsewhere [16,20] and are omitted here. Infrared lamps are used to raise and control the reactor temperature up to 400℃. Since most emission gases are exhausted at relatively high temperatures, it is indispensable to investigate the effect of temperature on the removal efficiency.

Result and Discussion

In addition to the malodorous gas found in crematory

Table 2 Odor control methods

Metho	Suitable condition	Advantage	Disadvantage
After-b rning (therm comb tion)	- Uniform furnace temperature (800-900 °C) - Residence time about 0.5~2 sec - Steady state operation	- Simple and widely available	- Unsuitable for unsteady state operation - Require sizable furnace
Catal reaction (catal comb tion)	- Known fixed gas species - Steady state operation	- Can be operated at relatively low temperature - High selectivity	- One catalyst can not simultaneously be effective for many species - Combustion is not good when the gas species change
Adsor on	- Relatively low temperature and space velocity - Steady and unsteady operation	- No problem with unsteady operation	- Regeneration is necessary - Relatively high pressure drop - Batch operation with multiple units
Gas ab rption	- Low to very high temperature - Steady and unsteady operation	- Can simultaneously remove particulate and odor	- Difficult to find the appropriate liquid absorbent - Complicated operation
Corona ischarge, includ electron attachi nt	- Low space velocity - Steady and unsteady operation	- Rapidly reach the steady state - Multiple removal mechanisms	- Relatively big reactor - High voltage

emission, the auth rs have investigated a wide variety of gas species. Tabl 3 summarized the types of gas species and the effect of v rious factors on their observed removal efficiencies. As a example, Table 3 reveals that the inlet concentration of (H3)2S to the reactor was investigated in the range 4-89 ppm; the concentration of coexisting O_2 from 0(nil) to 22 vol% and H_2O vapor from 600- 9,100 ppm. The identified reaction byproducts were SO_2 in the cases of coexisting O_2 alone and O_2 plus H_2O vapor. The removal efficiency of $(CH_3)_2S$ decreased as its inlet

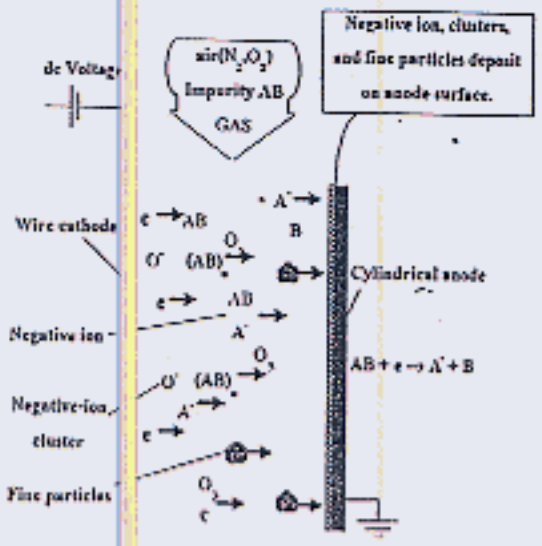

Figu 1 Principle of gas purification

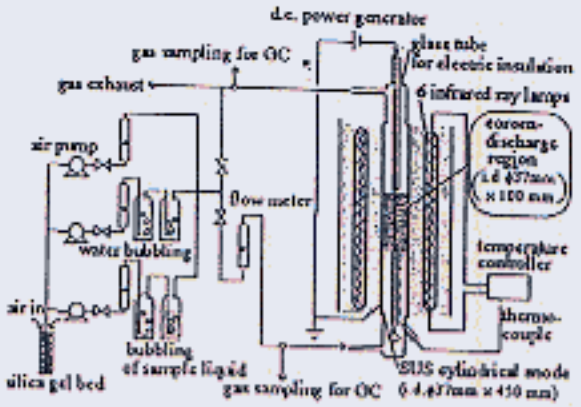

Figure 2. Experimental set-up for gas purification at high temperature

concentration ncreased. In contrast, when the concentration f coexisting O_2, H_2O vapor or both increased, the re oval efficiency of $(CH_3)_2S$ tended to rise. Moreover, the o served maximum removal efficiency of $(CH_3)_2S$ was hig r than 80% at 4 ppm (symbol A) in the case of pure N_2 oexisting O_2 or O_2 plus H_2O vapor. One can notice that e removals of most gases investigated here also show very high removal efficiency in the presence of oxy en. Obviously, the corona discharge reactor is applic ble to such malodorous crematory gas species as $(CH_3)_2$ N, H_2S, CH_3CHO, CH_3SH,$(CH_3)_2S$, SO_2 and so on.

Table 4 summ rizes the role of coexisting O_2. A wide range of removal echanisms can take place in the corona discharge reactor nd in several of them O_2 often enhances the removal ef ciency. To obtain good results the deposition on the node surface should be stable. Table 5 lists the main ch acteristics of the solid deposits. These tables contribute a better understanding of the dominant removal mechani n for each species.

Figure 3 shows an example of the effect of temperature on the removal o SO_2 at dry and humidified conditions. This figure shows that the removal efficiency of SO_2 decreases as the temperature increases and that H_2O vapor enhances the removal efficiency especially at low temperature condition.

Tanthapanichakoon et al.[9,10] have investigated the effect of reactor structure and come up with the following design guideline:

a. Whenever applicable, a thicker cathode wire should be used because it generally leads to higher removal efficiency.
b. For the same space velocity and reactor volume, a slender reactor has a higher removal efficiency than a stocky reactor.
c. Only a single cathode wire should be used in the reactor. The use of multiple cathodes has been shown to lead to a deterioration in the removal efficiency.

The authors have also investigated the simultaneous removal of a few pairs of gas species. However, they are omitted because of space limitation.

Conclusion

The corona discharge reactor has shown a good promise for the treatment of crematory emission. More development work, however, is necessary before its actual

Table 3. Effect of coexisting oxygen and water vapor in nitrogen on the reaction byproducts and removal efficiency

Sample Gas	Experimental conditions [1]				Reaction Byproduct	Removal efficiency								Ref No.
						Change of removal efficiency when the gas below increases				Maximum efficiency [2]				
	C_o (Sample gas) (ppm)	C_{O_2} [%]	C_{H_2O} (ppm)	SV (hr^{-1})		C_o (in N_2 Only)	O_2	H_2O	O_2 + H_2O	C_o (in N_2 Only)	O_2	H_2O	O_2 + H_2O	
SF_6	0.17-29	NI	NI	18.9	NI	↓	NI	NI	NI	A	NI	NI	NI	2,6
H_2S	60	NI	400-1,100	37.8	None	↓	NI	↑	NI	A	NI	A (80ppm)	NI	1,2,6
SO_2	32.7-30	0-16	400-13,000	18.9-37.8	None	↓	↑	↑	↑	C (33ppm)	A	D (122ppm)	A	1,2,6, 12
CS_2	50-65	0-40	300-11,000	18.9-37.8	SO_2 , COS	↓	↑ [4]	↑	↓	A (30ppm)	A	B (48ppm)	A	1,2,6
COS	20-53	0-50	650-10,000	18.9-37.8	SO_2	↓	↑ [4]	↑	NI	B	A	B (53ppm)	NI	1,2,6
CH_3SH	40-65	0-20	1,000-10,000	18.9-37.8	SO_2 , H_2S or COS	↓	↑	↑	NI	B	A	B (40ppm)	NI	1,2,6
$(CH_3)_2S$	3.88-65	0-22	600-9,100	18.9-52.9	SO_4^{--} , SO_3^{---}	↓	↑	↑	↑	A (4ppm)	A	D (30ppm)	A	1,2,6
CH_3I	75-85	5.6-8.0	5,600-17,600	47.3-50.0	I_2 (in N_2)	↓	↑	↑	↑	C	A	A	A	2,3,4
I_2	40.4-62	0-7	6,500	44-77.9	NI	NI	↑	↓	NI	B [5]	A	A (at I=0)	NI	4,5
$C_2Cl_2F_4$	50-40	0-20	NI	18.9	HCl or [illegible]	↓	↓	NI	NI	A	A	NI	NI	2,10, 11
CH_3CHO	9.9-35	0-20	0-103	60.9	NI	↓	↑	↑	NI	B	A	A	NI	2,7,9, 10
C_5H_5N (skatole)	2.4	0-20	10,000	43.5-189	NI	NI	↑	NI	↑	A	A	NI	A	7
C_6H_6 (benzene)	205-31	20-34	7,500	18.7-28.4	NI	NI	↑	NI	↑	D	A	NI	A	8
p-$C_6H_4Cl_2$ (p-dichloro benzene)	19-57	19-20	NI	20.6-45.6	NI	↓	↑	NI	NI	B	A	NI	NI	8
NH_3	49-14	0-20	3,268-6,415	75.6-189	NI	NI	↑	NI	↑	D	A	NI	A	9,12
$(CH_3)_3N$	58.6-69	0-20	NI	58.6-69.4	CH_3CHO, C_2H_5OH, $(CH_3)_2CO$ or CH_3NO_2	NI	↑	NI	NI	D	A	NI	NI	2,9, 12
NO	674-74	0-20	NI	75.6	NI	NI	NI	NI	NI	C	NI	NI	N	9
O_3 [3]	1.1-8.5	NI	NI	315-846.3	NI	NI	NI	NI	NI	D [5]	NI	NI	NI	6

* : byproduct observed with coexisting oxygen

** : byproduct observed with coexisting water vapor

*** : byproduct observed with both coexisting oxygen and water vapor

Unless stated otherwise , the same byproducts are observed for the same sample gas.

1) Current , I = 0.05 – 2.0 mA ; Voltage , V = 6.0 - 20.0 kV

2) Removal efficiency ; A > 80% , B 60-80% , C 40-60% , D< 40 %

3) Removed by welled – wall reactor.

4) Removed by sweep-out-type type reactor

5) Complete removal at O_2 > 2%

NI : not investigated

Table 4. Dominant removal mechanism in the presence of O_2

Removal mechanism	Influence of O_2 on removal efficiency	Deposition at anode	Example	Removal efficiency
Reaction with O_2	Increase	Stable	I_2 . CH_3I . C_5H_5N . CH_3CHO . $(CH_3)_3N$	High
Formation of ion clusters induced by O^-	Increase	Stable	SO_2 . CS_2 . COS . CH_3SH . $(CH_3)_2S$. CH_3CHO . CH_3I	High
Polycondensation by reaction with O^-	Increase	Stable	C_6H_6	High
Polycondensation by dissociative electron attachment	None	Stable	p-$C_6H_4Cl_2$	High
Dissociative electron attachment	Decrease	Stable	$C_2F_3Cl_3$	Low
Dissociative electron attachment	None	Unstable	F_2 . Cl_2	Low

*Electrons are attached to coexisting oxygen

Table 5 Deposit on anode surface in the presence of O_2

Sample gas	Feature of deposit
Sulfur compounds	Solid containing S compound
I_2	Yellow powder (I_4O_9)
CH_3I	Black particles (not identified)
$C_2F_3Cl_3$	Black particles containing F . Cl
C_6H_6 . p-$C_6H_4Cl_2$	Polycyclic aromatic compounds of high boiling point
CH_3CHO	Hard brown coating containing CH_3CHO
$(CH_3)_3N$	Carbon compounds of high boiling point

application. Since most of the previous studies were carried out at room temperature, the effect of high temperature on the removal efficiency should be investigated further. So should the simultaneous removal of several malodorous gas species commonly found in crematory emissions.

Acknowledgement

W. T., N. D. and S. C. receive partial financial support from Thailand Research Fund. H. T. and N. S. visited with them under the OECF-TJTTP scheme.

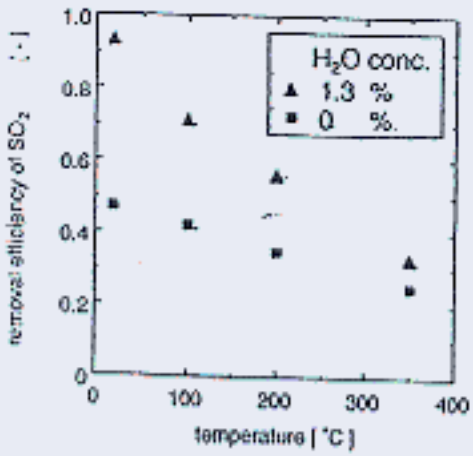

Figure 3. Removal efficiency of SO_2 from N_2-O_2 (-H_2O) mixture at various temperatures;
$[SO_2]_{in} = 4{,}000$ ppm , $[O_2] = 20\%$

Reference

1. Tamon, H., Sano, N. and Okazaki, M. " Influence of Oxygen and Water Vapor on Removal of Sulfur Compound by Electron Attachment," AIChE J., 1996, 42,p. 1481-1486.
2. Tanthapanichakoon, W., Larpsuriyakul, K., Khongpraserukal, P., Charinpanitkul, T., Tamon, H., and Okazaki, M." Basic Study on the Application of Electron Attachment Reaction to the Treatment of Crematory Emission Gas, " J. National Res. Council of Thailand, 1996, vol 28,pp.282-313.
3. Sano, N., Nagamoto, T., Tamon, H., Suzuki, T. and Okazaki, M." Removal of Methyl Iodide in Gas by Corona-Discharge Reactor," J. Chem. Eng. Japan,1997, vol 30, pp.944-946 .
4. Sano, N., Nagamoto, T., Tamon, H. and Okazaki, M." Removal of Iodine and Methyl Iodide in Gas by Wetted-Wall Reactor Based on Selective Electron Attachment," J. Chem. Eng. Japan, 1996, 29, pp.59-64.
5. Sano, N., Tamon, H. and Okazaki, M." Removal of Iodine in Gas by Corona-Discharge Reactor," J. Chem. Eng. Japan, 1996, 29,pp.59-64.
6. Tamon H., Mizota, H., Sano, N., Schulze, S. and Okazaki, M." New Concept of Gas Purification by Electron Attachment," AIChE J., 1995, 41, pp.1701-1711.
7. Sano, N., Nagamoto, T., Tamon, H., Suzuki, T. and Okazaki, M." Removal of Acetaldehyde and Skatole in Gas by Corona-Discharge," Ind. Eng. Chem. Res., 1997b, 36, pp.3783-3791.
8. Tamon, H., Imanaka, H., Sano, N., Okazaki, M. and Tanthapanichakoon, W." Removal of Aromatic Compounds in Gas by Electron Attachment," Ind. Eng. Chem. Res., 1998, 37,pp.2770-2774.
9. P. Khongphasamkarn," Removal of Trimethylamine Acetaldehyde and Ammonia Gases using Electron Attachment Reaction," Master's thesis, Chulalongkorn University, Bangkok, Thailand (1998), ISBN 974-639-484-3.
10. Tanthapanichakoon, W., Larpsuriyakul, K., Charinpanitkul, T., Sano, N., Tamon, H. and Okazaki, M. " Effect of structure of corona-discharge reactor on removal of dilute gaseous pollutants using selective electron attachment," J. Chem. Eng. Japan, 1998,vol 31

pp.7-13

11. Sano ,N. Tamon ,H and Okazaki , M. "Removal of Chlorofl rocarbon ,1,1,2-Trichloro-1,2,2-Trifluorc luane , in Gas by a Corona-Discharge Reactor," nd. Eng. Chem. Res., 1998, 37, pp. 1428-14
12. Tanthap ichakoon, W., Tamon, H., Khongpl samkaln, P., Sano, N., Charinpanitkul, T., and Oka ki, M. " Removal of Trimethylamine and Ammoni Using Electron Attachment Reaction," Journal c the Science Society of Thailand (Science Asia), 19 9, 1, pp. 57-63.
13. Caledon , G. E. A Survey of the Gas-Phase Negative Ion Kine s of Inorganic Molecules. Electron Attachm t Reactions. Chem. Rev., 1975, 75, 333-351.
14. Massey, H. Negative Ions. Cambridge Univ. Press, C bridge, England, 1976.
15. Massey, H. Atomic and Molecular Collisions. Taylor & rancis, London, 1979.
16. Nishida, and Matsuda Y. Malodor of exhaust gas from cre atory. J. Odor Control, 1981, 1-11 (in Japanese
17. Nishida, Malodor at Cremation Facility (Part I). PPM, 19 3, 3, 49-58 (in Japanese).
18. Nishida, Malodor at Cremation Facility (Part II). PPM, 19 4, 4, 51-59 (in Japanese).
19. Tamon, , Yano, H. and Okazaki, M. A New Method Gas Mixture Separation Based on Selective Electron ttachment. Kagaku Kogaku Ronbunshu, 1989, 15, 63-668.
20. Tanthap ichakoon, W., Larpsuriyakul, K., Sano, N., Tamon, and Okazaki, M. Effect of reactor structure on remov of methyl iodide and chlorofluorocarbon in gas using elective electron attachment. Proc. Regional ym. Chem. Eng. 1996, Jakarta, Indonesia, October 96, 3.2.1-3.2.14.
21. Sano, N. ukuoka, M., Kanki, T., Tamon, H., Tanthap chakoon, W. and Charinpanitkul, T. Influence f Temperature on Removal of Sulfur Dioxide d Benzene from Air by Corona Discharge Reactor. Proc. of Asia Pacific Conference on Sustainable Energy and Environmental Technologies, Hong Kong, Dec. 2000, 99-103.

[2000.5.19受稿, 2000.9.18採録]

Journal of Multidisciplinary Research

Vol.14, No.1 (Serial No.53) Spring 2001

CONTENTS

Published by : Multidisciplinary Research Council of Japan
2-14-3, Iwamoto-cho, Chiyoda-ku, Tokyo 101-0032, Japan

Influence of Temperature on SO_2 Removal Enhanced by Water Vapor Using a Corona-Discharge Reactor

By *Noriaki Sano**, *Seita Nishimura*, *Tatsuo Kanki*, *Hajime Tamon*, *Wiwut Tanthapanichakoon*, and *Tawatchai Charinpanitkul*

A reactor using d.c. corona discharge of negative polarity was applied to remove sulfur dioxide from an oxygen-nitrogen mixture in the presence or absence of water vapor for temperatures ranging from room temperature to 350 °C. It was observed that increasing the reactor temperature caused a decrease in the removal efficiency. Mixing water vapor with the process gas resulted in an increase of the removal efficiency. The effect of the presence of water vapor on improving the removal efficiency was significant under low temperature conditions, while it was relatively moderate under high temperature conditions. In addition, the solid deposit formed inside the reactor at two temperatures, room temperature and 200 °C, was analyzed with both a differential scattering calorimeter and an X ray diffractometer. The analysis indicated that SO_2 was ultimately converted to solid sulfur in both the presence and absence of water vapor in the gas flow.

1 Introduction

Recently, a variety of gas purification technologies using electric discharge have been widely researched, for example methods utilizing pulse-corona discharge [1–3], a ferroelectric packed bed reactor [4], the electron beam process [5], and so forth. Some of these have been successfully developed up to an industrial or commercial scale. One common feature in the above methods is the utilization of high-energy plasma to produce reactive radicals for nonselective decomposition of gaseous impurities. Hence, a variety of reaction byproducts are formed in such gas purification processes, especially when organic compounds are present in the treated gases. In contrast to these high-energy discharge processes, a low-energy discharge is often effective for gas purification [6]. The selective electron attachment reaction and ion cluster formation have been shown to be important in the gas purification mechanism using low-energy d.c. discharge. One important benefit of high selectivity is the smaller amount of reaction byproducts that are formed by the low-energy discharge processes compared to the high-energy ones.

Concerning the low-energy discharge process for gas purification, several types of d.c. corona-discharge reactors have been researched to remove sulfur compounds, organic compounds, nitrogen compounds and iodide compounds from air at room temperature [6–15]. In these previous articles, it has been found that admixing of water vapor was effective in enhancing the removal efficiency of some gaseous species from the air. It was postulated that the ion-induced formation of clusters in the discharge region would play an important role in the enhancement of the removal efficiency with the admixed oxygen and water vapor. In spite of the accumulated reports concerning the gas purification by corona discharge, however, the information on the influence of temperature on this enhancement effect has not been made available.

In this study, the d.c. corona-discharge was used to remove one of the common elements contained in the incineration exhaust gases, sulfur dioxide (SO_2), from a N_2-O_2 mixture in the presence or absence of water vapor at room temperature up to 350 °C. Additionally, the deposit formed inside the reactor was characterized to allow discussion of the removal mechanism.

2 Experimental

2.1 Temperature Effect on Removal of SO_2 from N_2-O_2 (-H_2O) Mixture

Fig. 1 shows the experimental set up employed to observe the temperature effect on the removal of SO_2 from a N_2-O_2-H_2O mixture.

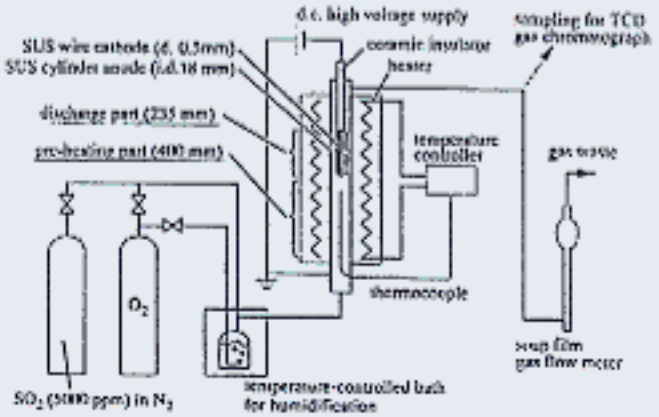

Figure 1. Apparatus to investigate the temperature effect on the removal of SO_2 from a N_2-O_2 mixture.

Standard gas containing 5000 ppm of SO_2 balanced with N_2 was used to supply SO_2. O_2 was mixed with the standard gas flow at 20 % to make a synthetic gas for the removal of SO_2, whose concentration at the inlet of the reactor was 4000 ppm. The O_2

[*] Dr. N. Sano (correspondence author, e-mail: sano@mech.eng.himeji-tech.ac.jp), Dipl. S. Nishimura, Prof. T. Kanki, Department of Chemical Engineering, Himeji Institute of Technology, 2167 Shosha, Himeji 671-2201, Japan; Prof. H. Tamon, Dpartment of Chemical Engineering, Kyoto University, Kyoto 606-8501, Japan; Prof. W. Tanthapanichakoon, Dr. T. Charinpanitkul, Department of Chemical Engineering, Chulalongkorn University, Patumwan, Bangkok 10330, Thailand.

gas was humidified by ubbling through distilled water set in a temperature controlle bath when the influence of coexisting water vapor was to be bserved. A corona-discharge reactor, which consisted of grounded cylindrical SUS anode (i.d.=18 mm) and a w e cathode (d.= 0.5 mm), was used to remove SO_2 from the s flow of 2.0×10^{-6} $m^3 s^{-1}$. A d.c. high voltage of negative pol rity was applied to the wire cathode to generate the corona di charge. The reactor was heated by an electrical furnace wrap ed around the anode, and the temperature of the reactor w controlled up to 350 °C using a PID controller. The reactor was separated into two parts; the first part (400 mm) without corona discharge was for pre-heating the gas flow and the secon part (235 mm) was for the removal of SO_2 by the corona disch rge. The temperature profile inside the second part was mea ured and it was ensured that the temperature gradient i the axial direction was negligible. The concentration of SO_2 a he outlet of the reactor was measured by a gas chromatograp with a thermal conductivity detector (TCD) (Shimadzu, GC BT). The adsorbent used for the GC column was 1,2,3 Tris 2-(Cyanoethoxy)] Propane 25 % on Shimalite (GL Sciences nc.).

2.2 Analysis of Deposi Formed in the Reactor

In order to discuss th removal mechanism, it is necessary to characterize the solid deposit formed inside the reactor. For this purpose, a corona discharge reactor with a detachable plate anode was built, illustrated in Fig. 2.

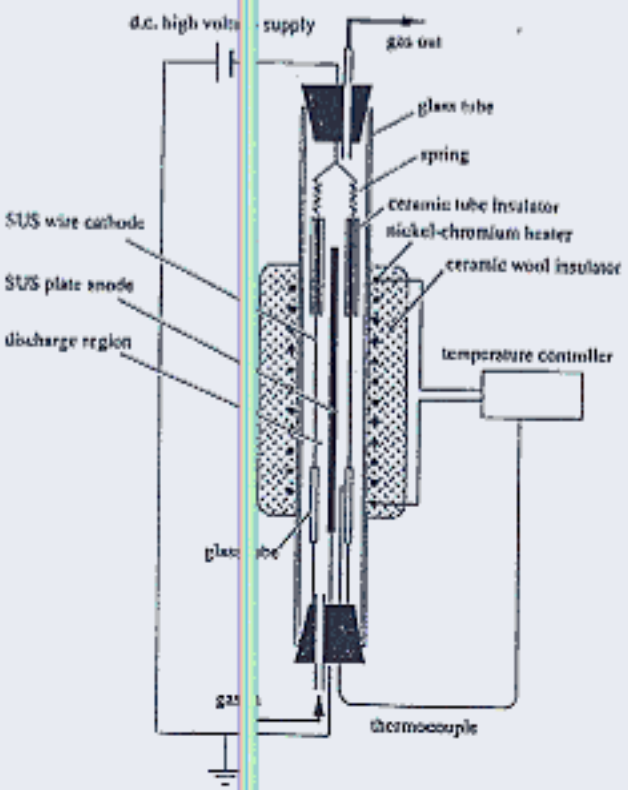

Figure 2. Reactor with plate-sh e anodes to collect the deposit formed inside the reactor during the removal SO_2 at various temperatures.

The reactor vessel was a glass tube inserted in an electronic furnace. Two wire cathodes were set apart on opposite sides of a plate anode, and the corona discharge region was limited inside the furnace. The deposit formed inside the reactor was characterized by a differential scanning calorimeter (DSC) (DSC-22, Seiko Instruments Inc.) and an X-ray diffractometer (RIGAKU DENKI Co. Ltd., RINT1500).

3 Results and Discussion

3.1 Removal Efficiency of SO_2 in the Presence or Absence of Water Vapor

It is known that the voltage required to generate the corona discharge decreases with the temperature elevation. Under our experimental condition, 5.5 kV was required to obtain 0.4 mA at room temperature, and it decreased gradually down to 4.0 kV at 350 °C. Fig. 3 shows the influence of the reactor temperature on the removal efficiency of the SO_2 from N_2-O_2 and N_2-O_2-H_2O mixtures.

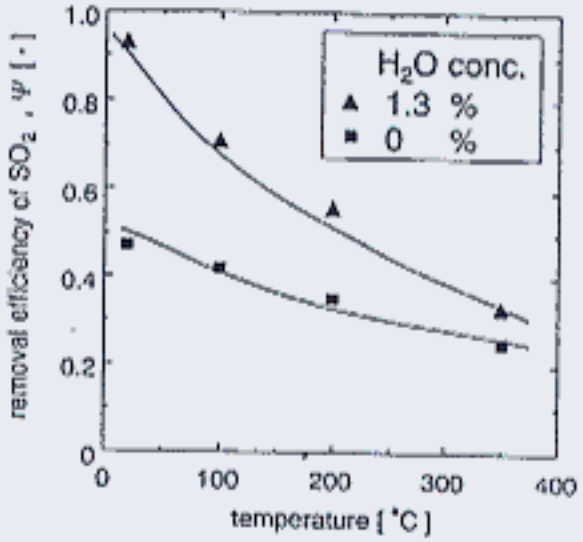

Figure 3. Removal efficiency of SO_2 from N_2-O_2 (-H_2O) mixture at various temperatures: $[SO_2]_{inlet} = 4000$ ppm, $[O_2] = 20$ %, gas flow rate = $2.0 \cdot 10^{-6}$ $m^3 s^{-1}$, current = 0.4 mA.

The removal efficiency Ψ is defined as the ratio of the concentration decrease of SO_2 to the inlet concentration of SO_2 as in Eq. (1)[1].

$$\Psi = (C_{in} - C_{out})/C_{in} \quad (1)$$

There was no reaction byproduct detected by the TCD gas chromatograph. If a detectable concentration of some unknown sulfur compound had been produced as a reaction byproduct, a TCD peak should have appeared with the GC column used in this study [6,7]. Then Ψ defined here represents the removal efficiency of the total sulfur. As a result, it was found that the removal efficiency of SO_2

1) List of symbols at the end of the paper.

significantly decreased ith increasing the reactor tempera-
ure in both the N_2-O_2 a d N_2-O_2-H_2O mixtures.

One can see in Fig. that the removal efficiency shows
significant enhancement n the presence of water vapor. This
esult is consistent with previous article [7]. It is interesting
hat the enhancement e ct by water vapor on SO_2 removal
decreased as the reactor emperature rose.

The electron efficien η, the mean number of removed
SO_2 molecules per one ectron, is defined in Eq. (2) as the
atio of removed SO_2 mo ecules to the number of the electron
harges emitted in the d charge current.

$$\eta = (QC_{in}\Psi)/(IF) \quad (2)$$

where Q, C_{in}, Ψ, F, and I re respectively gas flow rate [mol/s],
nlet concentration of O_2 [mol fraction, -], the removal
fficiency [-], Faraday co stant [coulomb/mol], and discharge
current [A]. When SO_2 s removed at room temperature, η
was estimated as 30 an 58 at 0 % and 1.3 % of the H_2O
concentration respective . When the temperature was raised
to 350 °C, η was estimate as 16 and 21 respectively at 0 % and
1.3 % of the H_2O concen ation. These results suggest that the
enhancement effect of t presence of H_2O on the removal
efficiency decreases fron a factor of 1.9 at room temperature
to 1.3 at 350 °C.

3.2 Influence of the Reac or Temperature on the Removal Mechanism

Under the conditions f the corona discharge inside the
reactor, the dissociative ctron attachment shown in Eq. (3)
appeared dominant am ng the several types of electron
ttachment reactions, wi n the estimated magnitude of the
lectron energy (>0.3 e was considered. In addition, the
stimated rate of the diss ciative electron attachment of SO_2
negligible compared wi that of O_2 because the concentra-
ion of O_2 is much highe than that of SO_2 [6]. The electron
ttachment to produce O_2^- as shown in Eq. (4) may be
significant because t electron energy level may be
xcessive for this reac on [16,17]. Hence, the electron
ttachment to O_2 for pr lucing O^- can be considered as an
mportant scheme for the emoval mechanism here.

$$e + O_2 \rightarrow O^- + O \quad (3)$$

$$e + O_2 \rightarrow O_2^- \quad (4)$$

Following the producti of O^- and O, the reactions of SO_2
with O^- and O would b considered to contribute to the
emoval of SO_2. Concern g the influence of temperature on
he dissociative electron a achment to O_2, it was reported that
he dissociative electron tachment rate increased when the
emperature was increas [17]. However, the result in this
tudy showed that the re oval efficiency of SO_2 decreased
despite the increased production rates of O^- and O at the elevated temperature. In order to understand why the removal of SO_2 decreases with the temperature elevation, the temperature dependency of the reaction rates of SO_2 with O^- and O requires further investigation.

When negative ions are produced in the O_2-SO_2 mixture, the coulomb force between the ions and other susceptible molecules may induce ion-nucleated clusters. Moruzzi et al., detected the negative ion O^- and its clustering of SO_2, $O^-[SO_2]_n$ (n = 1 to 3), when they measured the electron attachment reaction rate of an O_2-SO_2 mixture by the drift tube method [18]. Tamon et al. reasoned that these ion clusters played an important role in the high removal efficiency of SO_2 from the air, in which single-charged ion clusters containing multiple SO_2 molecules would react with the anode surface to form a solid deposit, thus resulting in the simultaneous removal of several SO_2 molecules by one electron [7]. We consider that this positive effect of the cluster formation is retarded by temperature elevation because these ion clusters are expected to be less stable, since individual molecules become more energetic at high temperature.

Concerning the effect of coexisting water vapor, Moruzzi et al. reported their experimental observation that the negative ion O^- and its clustering with H_2O, $O^-[H_2O]_n$ (n = 1 to 5), were produced when electrons were introduced to H_2O-O_2 mixture [16]. Therefore it is logical to postulate the formation of O^--nucleated ion clusters with both H_2O and SO_2 molecules, $O^-[H_2O]_n[SO_2]_m$, in the discharge region during the removal of SO_2 from a gas containing H_2O and O_2. Tamon *et al.* reported that when these clusters drifted to the anode surface, they were converted to solid deposit there. In conclusion, the mechanism of cluster formation can be deduced to be one of the reasons for the enhancement effect on the removal of SO_2 by admixing H_2O [7]. Furthermore, the negative ion clusters would probably grow to become aerosol particles with additional absorption of SO_2, thus resulting in the enhanced transfer of SO_2 to the anode surface.

On the other hand, Morruzi *et al.* also mentioned that the concentration of the clusters produced in their experiments decreased when the temperature increased [16]. This indicates that the instability of the ion cluster at high temperature is one of the reasons for the reduced enhancement of SO_2 removal by water vapor. The enhancement of the removal by the aerosol particles should also decrease with the temperature elevation.

3.3 Analysis of the Deposit on the Anode Surface

An SO_2-O_2-H_2O mixture ($[SO_2]$ = 2500 ppm, $[O_2]$ = 50 %, $[H_2O]$ = 0.3 %]) was introduced to the plate-anode reactor described in Fig. 2 with a discharge current 1.0 mA (1.5 kV) at room temperature, and a deposit was formed on the anode surface. The deposit was initially a wet film, and it turned into yellow powder upon drying. The spectrum of the dried powder obtained with the X-ray diffractometer is shown in Fig. 4.

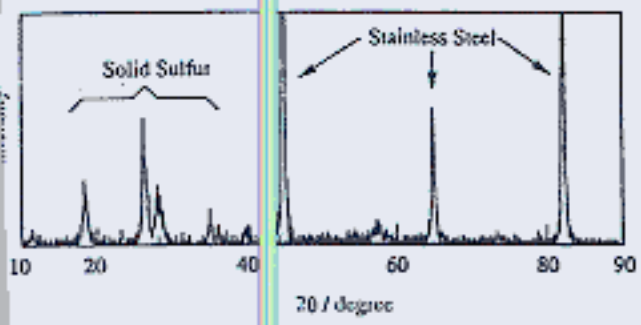

ure 4. X-ray diffraction patte of the deposit formed on the anode surface: $O_2]_{in}$ = 2500 ppm, $[O_2]$ = 50 , $[H_2O]$ = 0.3 %, room temperature for the osit formation condition.

This spectrum pattern dicates that the powder contains lfur solid. Interestin y when the d.c. discharge was nerated in the reacto at the elevated temperature of 00 °C, the deposit would ot accumulate on the heated part of e reactor. Instead the ellow powder was formed on the alls outside the heated art. Nevertheless the same X-ray ffraction spectrum was lso obtained from this powder.

When this powder was nalyzed with a differential scanning lorimeter (DSC), two endothermic peaks at 103 °C and 20 °C and an exotherm peak at 320 °C were detected as own in Fig. 5.

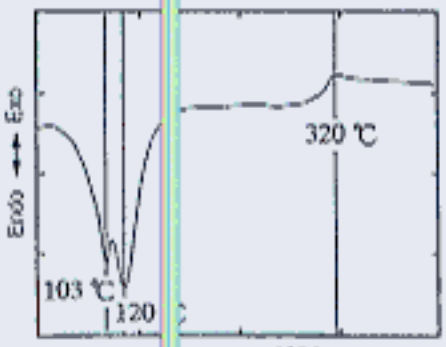

ure 5. DSC spectrum of dep it formed on the anode surface; $[SO_2]_{in}$ = 0 ppm, $[O_2]$ = 50 %, $[H_2O$ = 0.3 %, room temperature for the deposit mation condition.

The endothermic peak t 103 °C is thought to come from the aporation of residual ater contained in the sample. The dothermic peak at 12 °C should be the melting point of onoclinic (β-) sulfur so d. The phenomenon related to the othermic peak at 320 C has not been identified yet. From ese results, one can confirm that SO_2 is ultimately composed to sulfur so d in the discharge region.

The reason why the su ur particles were formed on the cold ody inside the reactor c uld be explained as follows. Initially e elemental sulfur sho ld have been produced on the hot node at 200 °C as in e case of room temperature. The aximum possible part l pressure of sulfur gas assuming omplete conversion fron SO_2 in the discharge region would be ss than 253 Pa because e inlet concentration of SO_2 in Fig. 2 was 2500 ppm at room temperature, which is equivalent to 253 Pa of SO_2. However, the vapor pressure of the liquid sulfur at 200 °C is 280 Pa. In this condition, any sulfur deposit formed on the heated anode cannot remain condensed. When the sulfur vapor diffuses to the cold region along with the convection of the gas flow, the sulfur can readily condense on the walls because the vapor pressure of the solid sulfur at 50 °C is 0.027 Pa.

4 Conclusion

A d.c. corona-discharge reactor was applied to remove SO_2 from O_2-N_2 and O_2-N_2-H_2O mixtures. In order to investigate the temperature effect on the removal efficiency of SO_2, the temperature of the reactor was controlled to various constant temperatures, from room temperature to 350 °C. We have confirmed that the elevation of the reactor temperature caused a decrease of the removal efficiency in both the removal of SO_2 from O_2-N_2 and O_2-N_2-H_2O mixtures, and the removal efficiency was improved by admixing water vapor. The results revealed that this enhancement of SO_2 removal by water vapor significantly decreased when the temperature was increased.

Additionally, the deposit which formed inside the reactor during the removal of SO_2 at room temperature and 200 °C, was characterized using an X ray diffractometer and a differential scanning calorimeter. It is found that the deposit contained solid sulfur. When the removal of SO_2 was carried out at room temperature, the deposit of sulfur was formed on the anode surface. In contrast, when the reactor temperature was 200 °C, the sulfur deposit would not remain on the heated anode but it vaporized and condensed on the low-temperature section.

Acknowledgement

Financial supports by the grants from the Himeji Kogyo Daigaku Koen Zaidan foundation (1998–1999) to N. S., from Thailand Research Fund to W. T. and T. C. and from OECF Thailand-Japan Technology Transfer Project (TJTTP-OECF) at Chulalongkorn University (1999-2000) are greatly acknowledged.

Received: February 12, 2001 [CET 1369]

Symbols used

C_{in}	[–]	inlet concentration of SO_2
C_{out}	[–]	outlet concentration of SO_2
F	[coulomb/mol]	Faraday constant
I	[A]	discharge current
Q	[mol/s]	gas flow rate
Ψ	[–]	removal efficiency defined by Eq. (1)

References

[1] Masuda, S.; Nakano, H., *...ntrol of NOx by Positive and Negative Pulsed Corona Discharges*, I... EE-IAS Annual Meeting, Denver 1986, pp. 1173–1182.

[2] Mizuno, A.; Shimizu, K., ...Matsuoka, T.; Furuta, S., *IEEE-IAS Transactions. 31* (1995) No 6, pp. ...1463–1467.

[3] Yang, C. L., *Env. Prog.* ... (1999) No 2, pp. 80–86.

[4] Yamamoto, T.; Chang, ... S.; Berezin, A. A.; Kohno, H.; Honda, S.; Shibuya, A., *J. Adv. Oxi...* *Technol. 1* (1996) No 1, pp. 67–78.

[5] Kawamura, K., *Kagaku ...logaku, 53* (1989) p. 820.

[6] Tamon, H.; Mizota, H.; ... no, N.; Schulze, S.; Okazaki, M., *AIChE J. 41* (1995) No 7, pp. 1701–1... .

[7] Tamon, H.; Sano, N.; ...Okazaki, M., *AIChE J. 42* (1996) No 5, pp. 1481–1486.

[8] Sano, N.; Nagamoto, T.; ...mon, H.; Okazaki, M., *J. Chem. Eng. Japan, 29* (1996) No 1, pp. 59–6...

[9] Sano, N.; Nagamoto, T.; ...mon, H.; Suzuki, T.; Okazaki, M., *J. Chem. Eng. Japan 30* (1997) No ..., pp. 902–909.

[10] Sano, N.; Tamon, H.; Okazaki, M., *J. Chem. Eng. Japan 30* (1997) No 5, pp. 944–946.

[11] Sano, N.; Nagamoto, T.; Tamon, H.; Suzuki, T.; Okazaki M., *Ind. Eng. Chem. Res. 36* (1997) No 9, pp. 3783–3791.

[12] Tanthapanichakoon, W.; Laupsuriyakul, K.; Charinpanitkul, T.; Sano, N.; Tamon, H.; Okazaki, M., *J. Chem. Eng. Japan 31* (1998) No 1, pp. 7–13.

[13] Sano, N.; Tamon, H.; Okazaki, M., *Ind. Eng. Chem. Res. 37* (1998) No 4, pp. 1428–1434.

[14] Tamon, H.; Imanaka, H.; Sano, N.; Okazaki, M.; Tanthapanichakoon, W., *Ind. Eng. Chem. Res. 37* (1998) No 7, pp. 2770–2774.

[15] Tanthapanichakoon, W.; Khongprasamkaln, P.; Charinpanitkul, T.; Tamon, H.; Sano, N.; Okazaki, M., *Science Asia 25* (1999) No 1, pp. 57–63.

[16] Moruzzi, J. L.; Phelps, A. V., *J. Chem. Phys. 45* (1966) 4617–4627.

[17] Massey S. H., *Negative Ions*, Cambridge Univ. Press, Cambridge, U.K., 1976.

[18] Lukdawala, V. K.; Moruzzi, J. L., *J. Phys. D: Appl. Phys. 14* (1981) pp. 2015–2026.

Removal of Trimethylamine in Gas by Corona-Discharge Reactor

HAJIME TAMON[1], YOSHIHITO SUEOKA[1],
NORIAKI SANO[2], WIWUT TANTHAPANICHAKOON[3],
PAISARN KHONGPRASARNKALN[3]
AND TAWATCHAI CHARINPANITKUL[3]

[1]*Department of Chemical Engineering, Kyoto University, Kyoto 606-8501, Japan*
[2]*Department of Chemical Engineering, Himeji Institute of Technology, Himeji 671-2201, Japan*
[3]*Department of Chemical Engineering, Chulalongkorn University, Patumwan, Bangkok 10330, Thailand*

Reprinted from
JOURNAL OF
CHEMICAL ENGINEERING
OF
JAPAN
Vol. 34, No. 8 (2001)
Pages 1006–1011

Literature Cited

Hanai, T., A. Kakam… H. Honda, T. Furuhashi, Y. Uchikawa and T. Kobayashi; "M… deling of Total Evaluation Process of *Ginjo Sake* Using a Fuz… Neural Network," *Trans. SICE.*, 32, 1113–1120 (1996)

Hanai, T., S. Hibino… E. Nagata, M. Matsubara, K. Fukagawa, T. Shirataki, H. H… nda and T. Kobayashi; "Assessment of Senile Dementia of … zheimer Type Using Artificial Neural Networks," *Japan. J. … Medical Electron. Biol. Eng.*, 37, 178–183 (1999)

Honda, H. and T. K… ayashi; "Fuzzy Control of Bioprocess," *J. Biosci. Bioeng.*, 89, 401–408 (2000)

Honda, H., T. Hanai, … Katayama, H. Tohyama and T. Kobayashi; "Temperature Co… trol of Ginjo Sake Mashing Process by Automatic Fuzzy … Modeling Using Fuzzy Neural Networks," *J. Ferment. Bioen…*, 85, 107–112 (1998)

Horikawa, S., T. Furu… shi and Y. Uchikawa; "A Study on Fuzzy Modeling Using … zzy Neural Networks," Proc. of IFES'91, pp. 562–573, Yok… ama, Japan (1991)

Matsuyama, Y.; "Har… ful Effect of Dinoflagellate *Heterocapsa circularisquama* … Shellfish Aquaculture in Japan," *JARQ—Japan Agricultura… Research Quarterly*, 33, 283–293 (1999)

Nakanishi, K., T. Ma… ida, N. Hata, T. Morita, K. Takayanagi, K. Abo and T. Uchida; Akashio Taisaku Gijutu Kaihatsu Shiken Houkoku, p. 1, Mie-ken Suisan Gijutu Center, Mie, Japan (1998) (in Japanese)

Noguchi, H., T. Hanai, W. Takahashi, T. Ichii, T. Tanikawa, M. Masuoka, H. Honda and T. Kobayashi; "Model Construction for Quality of Beer and Brewing Process Using FNN," *Kagaku Kogaku Ronbunshu*, 25, 695–701 (1999) (in Japanese)

Okaichi, T., ed.; Akashio no Kagaku, 2nd ed., Kouseisha Kouseikaku, Tokyo, Japan (1997) (in Japanese)

Ouchi, A.; "Simulation of Red Tide by Means of Multiple Regression and Fourier Analysis," *Bull. Japan. Soc. Sci. Fish.*, 52, 203–207 (1985)

Rumelhart, D. E., G. E. Hinton and R. J. William; "Learning Representations by Back-Propagating Errors," *Nature*, 323, 533–536 (1986)

Shioya, S., K. Shimizu and T. Yoshida; "Knowledge-Based Design and Operation of Bioprocess Systems," *J. Biosci. Bioeng.*, 87, 261–266 (1999)

Suga, T.; Taheenryou Kaiseki no Jissen, Gendai-Sugakusha, Kyoto, Japan (1993) (in Japanese)

Tomida, S., T. Hanai, N. Ueda, H. Honda and T. Kobayashi; "Construction of COD Simulation Model for Activated Sludge Process by Fuzzy Neural Network," *J. Biosci. Bioeng.*, 88, 215–220 (1999)

Journal of Chemical Engineering of Japan, Vol. 34, No. 8, pp. 1006–1011, 2001

Removal of Trimethylamine in Gas by Corona-Discharge Reactor

HAJIME TAMON[1], YOSHIHITO SUEOKA[1],
NORIAKI SANO[2], WIWUT TANTHAPANICHAKOON[3],
PAISARN KHONGPRASARNKALN[3]
AND TAWATCHAI CHARINPANITKUL[3]

[1]*Department of Chemical Engineering, Kyoto University, Kyoto 606-8501, Japan*
[2]*Department of Chemical Engineering, Himeji Institute of Technology, Himeji 671-2201, Japan*
[3]*Department of Chemical Engineering, Chulalongkorn University, Patumwan, Bangkok 10330, Thailand*

Keywords: Gas Purification, Corona-Discharge Reactor, Electron Attachment, Removal of Trimethylamine, Deposition

Trimethylamine, the component of malodorous gases from crematory emission, was removed by a corona-discharge reactor to apply the reactor to purification of crematory emission gas. The effects of discharge current and coexisting oxygen or water vapor on the removal efficiency of trimethylamine were investigated. Although trimethylamine was not effectively removed from nitrogen by corona discharge, the removal efficiency was improved greatly by mixing oxygen or water vapor. The amounts of reaction by-product generated were extremely large at high discharge current in the removal from a nitrogen-oxygen mixture. On the other hand, the by-products were greatly suppressed by mixing water vapor. The deposit on the anode of the reactor was analyzed by a thermogravimetry. As a result, trimethylamine was found on the anode surface as the deposit of carbon compounds which have high boiling point.

Introduction

Removal of volute malodorous gases has environmental and industrial significance. Most countries have been facing many environmental problems associated with the unceasing growth of human activities. For instance, a latent source of public nuisance emitted from the crematory furnace of a temple has become prominent in Thailand (Tanthapanichakoon *et al.*, 1999). Besides particulate, malodorous gaseous components are emitted during cremation, causing frequent complaints from surrounding communities. This is because the exhaust gas is directly released to the atmosphere from the stack without any treatment. Out of more than 30,000 temples all over Thailand, only a few big ones in Bangkok employ some sort of emission control devices, mainly, an after-burning chamber. A good crematory furnace system is usually imported and costs ca. 150,000 dollars nowadays. From on-site surveys at a number of temples in Bangkok, the locally made after-burning systems are too small, resulting in inadequate residence time, and their operating temperature is too low at 550–650°C (Tanthapanichakoon *et al.*, 1999).

Although the problem is much less severe, similar complaints about crematory emission are heard in Japan. To meet the emission control standards, a typical modern Japanese crematorium generally installs an after-burner furnace to decompose the malodorous organic gaseous components at high temperature. Next fresh air is drawn to cool down and further dilute the residual gaseous components by one or two orders of magnitude before sending the cooled-down gas through a dust collector (Nishida and Matsuda, 1981; Nishida, 1988a, 1988b).

It has been reported that malodorous and even noxious gases, such as trimethylamine ($(CH_3)_3N$), ammonia (NH_3), acetaldehyde (CH_3CHO) and styrene ($C_6H_5CH_2CH_3$), etc., are produced during cremation (Nishida, 1988a, 1988b). Often their concentrations are diluted with fresh air down to several tens or hundreds of ppm before leaving the stack. Because of greater public awareness and concern on air quality, the removal of malodorous gases from crematory emission has become a national issue. This has motivated the authors to jointly carry out a basic study on the application of a corona-discharge reactor to the treatment of crematory emission gas.

The authors have used two types of corona-discharge reactors to remove sulfur compounds, iodine and oxygen from nitrogen (Tamon *et al.*, 1995). They also discussed the removal mechanism and presented

Received on November 29, 2000. Correspondence concerning this article should be addressed to H. Tamon (E-mail address: tamon@cheme.kyoto-u.ac.jp).

simulation mod s for predicting the removal efficiency. Subseque tly, the authors investigated the influence of coexi ing oxygen and/or water vapor on the removal of s veral sulfur compounds (Tamon *et al.*, 1996). Then t e authors applied a corona-discharge reactor to remov of iodine compounds, chlorofluorocarbon (CFC), v latile organic compounds (VOCs), aromatic compo ds, etc. (Sano *et al.*, 1996, 1997a, 1997b, 1997c; Ta non *et al.*, 1998; Tanthapanichakoon *et al.*, 1999).

Figure 1 ill strates the principle of gas purification. High dc vo age is applied to a cylindrical reactor. The cathode i a stainless steel (SUS) wire stretched at the center of t e reactor and the anode is the outer cylinder. Electro s are produced by corona discharge and drift to the a ode in the electric field. During their drift, a part of th m collides with electronegative impurities and nega ve ions are produced. This phenomenon is called ele tron attachment (Massey, 1976). The impurities are co verted to negative ions, negative-ion clusters, or fine articles by electron attachment and removed by depo iting at the anode.

Some impu ties are, however, decomposed by corona discharge and reaction by-products are generated. The by-pro ucts seriously influence the applicability of corona- ischarge reactor to gas purification. The deposition m chanism is also not fully understood. The analysis of t e deposit on the anode surface is indispensable to el cidate the mechanism. Since the removal mechanis by corona-discharge depends on the properties of the impurities, it is necessary to obtain fundamental dat such as the removal efficiency, the formation of re ction by-product, the deposition mechanism, etc. o successfully apply the reactor to the removal of m odorous gases from crematory emission. Hence, the urpose of this work is to elucidate the formation of action by-products and suppress the formation in the emoval of $(CH_3)_3N$.

In this artic , a corona-discharge reactor is applied to the remo al of dilute $(CH_3)_3N$. The formation of reaction by-p ducts in the reactor is discussed for the removal fron N_2, N_2-O_2, N_2-H_2O, and N_2-O_2-H_2O. Then the deposit the anode of the reactor is analyzed.

1. Experimen al

1.1 Removal ex eriment

The experim ental set-up was reported in the previous articles (T mon *et al.*, 1995; Sano *et al.*, 1996). A brass pipe was used as the anode whose inner diameter and length w re respectively 38 mm and 280 mm. The cathode wa SUS wire whose diameter was 0.3 mm. Except the e ectrodes the vessel of the reactor was acrylic resin an the cathode was sustained by a ceramic insulator c the top and by Teflon threads on the bottom. A dc vo age of −3 to −25 kV was applied to the cathode to g erate corona discharge.

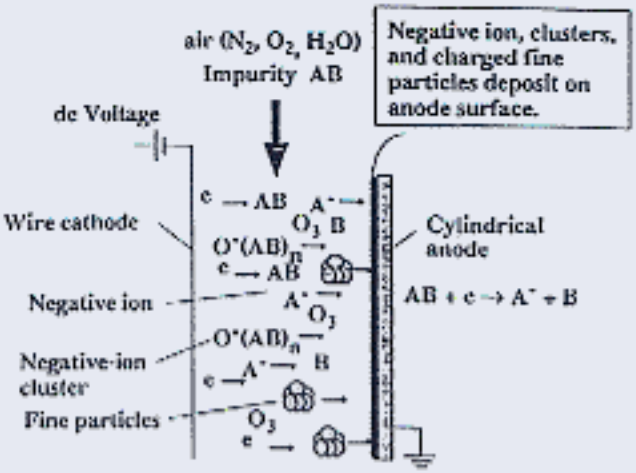

Fig. 1 Gas purification principle

The concentration of $(CH_3)_3N$ was adjusted by mixing a commercial standard gas with a balance gas, N_2. The concentration of H_2O was controlled by bubbling N_2 through distilled water in a temperature-controlled bath.

The concentrations of $(CH_3)_3N$ at the inlet and the outlet of the reactor were measured by a gas chromatograph (GC-14B, Shimadzu Corporation) with a flame ionization detector (FID). When unknown reaction by-products were detected on a gas chromatogram, a gas chromatograph mass spectrometer (GCMS) (MS-QP1000S, Shimadzu Corporation) was used to identify the reaction by-products. The peak areas of reaction by-products generated in the reactor were measured by FID. Although the calibration of peak areas was needed to determine the concentrations of by-products strictly, the concentrations were approximately calculated by comparing those peak areas with that of $(CH_3)_3N$ based on the assumption that the peak sensitivity for all compounds is the same. The concentration of H_2O was measured by a dew point hygrometer (MODEL 2586, Yokogawa Electric Corporation).

1.2 TG analysis of anode surface

In the present corona-discharge reactor, a deposit is formed on the anode surface during a removal experiment. An analysis of the deposit should be useful to understand the removal mechanism. To analyze the deposit at the anode, the authors constructed a reactor that had two detachable plate anodes (Sano *et al.*, 1997c). The reactor had two 50 × 200 mm plate anodes paralleled with 50 mm gap and a wire cathode of 0.3 mm diameter was stretched in the center of those anodes. The deposit was analyzed by a thermogravimetric (TG) analyzer (TG-8120, Rigaku Co. Ltd.).

2. Results and Discussion

2.1 Removal of $(CH_3)_3N$ from N_2

To evaluate the removal of $(CH_3)_3N$ by the corona-discharge reactor, the definition of removal efficiency,

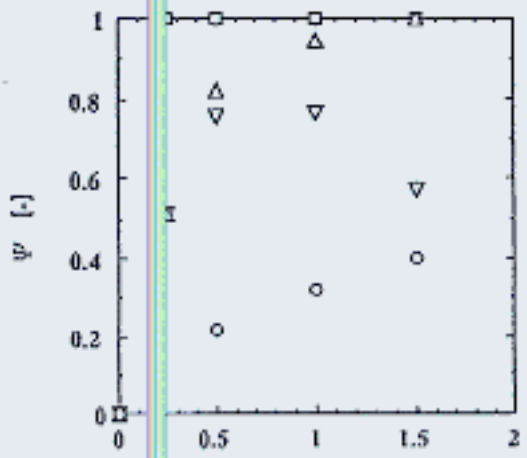

	C_{in} [ppm]	C_{O_2} [%]	C_{H_2O} [ppm]	Q [cm³/min]
○	26	0	0	335
△	28	0	4950	360
▽	25	0	10000	443
□	29	19	0	419

Fig. 2 emoval efficiency of $(CH_3)_3N$

Ψ, used in this w rk is as follows.

$$\Psi = 1 - C_{out}/C_{in} \quad (1)$$

Figure 2 sh vs the removal efficiency of $(CH_3)_3N$ from N_2 (circula dots). Ψ obviously increases as the discharge curren I increases. This is because the concentration of elec rons drifting in the reactor increases with increasing I. In the removal, however, Ψ is quite low. Methane (C_4) generated in the reactor was identified as a reactio by-product by GCMS. CH_4 constituted about 7% the inlet concentration of $(CH_3)_3N$ at 1.5 mA discha ge current. Hence, the authors consider that $(CH_3)_3$ is decomposed by corona discharge and a polyconde sation reaction occurs. However, the authors cannot e plain the reaction mechanism in the present stage of vestigation.

2.2 Removal of $(CH_3)_3N$ from N_2-O_2

Since the a ual removal process often contains O_2 and H_2O, it i imperative to investigate the influence of O_2 and H O on the removal of gas impurities. Figure 2 also sh ws the experimental results on the removal of $(CH_3)_3N$ with 19% O_2 (square dots). When the discharge cu ent was as little as 0.25 mA, $(CH_3)_3N$ disappeared in th FID detection. Thus the presence of O_2 greatly enhar ed Ψ. To explain such high removal efficiency, the a thors have studied the role of ozone (O_3) (Tanthapan hakoon *et al.*, 1999). This research proves conclus ely that the enhanced removal of $(CH_3)_3N$ can be tributed to the O_3 reaction.

Table 1 List of reaction by-products generated in removal of $(CH_3)_3N$ from N_2-O_2 mixture

Retention time [min]	M/Z	M/Z of fragment	By-product
1.7	44	43, 42, 29, 28, 27	CH_3CHO
3.3	46	45, 44, 30, 31, 29	C_2H_5OH
4.9	58	57, 42, 29, 28, 27	$(CH_3)_2CO$
6.9	61	60, 46, 45, 30, 29	CH_3NO_2

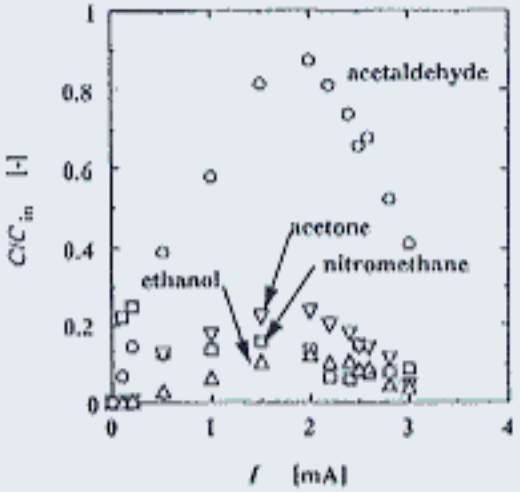

Fig. 3 Reaction by-product in removal of $(CH_3)_3N$ from N_2-O_2 (C_{in} = 29 ppm, C_{O_2} = 19%, Q = 419 cm³/min)

Reaction by-products were identified by GCMS as listed in **Table 1**. Acetaldehyde (CH_3CHO), ethanol (C_2H_5OH), acetone ($(CH_3)_2CO$), and nitromethane (CH_3NO_2) were observed as the by-products. Although it seems that organic acids are generated during an oxidation process of $(CH_3)_3N$, the acids have not been detected by GCMS. Since the removal efficiency of $(CH_3)_3N$ is greatly improved by the O_3 reaction, the by-products are considered to be generated by the O_3 reaction with $(CH_3)_3N$. **Figure 3** shows the amounts of the by-products generated in the corona-discharge reactor. The ordinate indicates the mole ratio of the by-products generated in the reactor to the inlet concentration of $(CH_3)_3N$, C/C_{in}, and the abscissa the discharge current, I. C/C_{in} for CH_3CHO is ca. 0.9 at 2.0 mA discharge current. In this case $(CH_3)_3N$ changes to CH_3CHO by corona discharge and the reactor cannot be applied to the removal of $(CH_3)_3N$. Since $(CH_3)_3N$ is decomposed by reaction with O_3, the total molar concentration of reaction by-products is sometimes more than the inlet concentration of $(CH_3)_3N$, C_{in}. The amount of the by-products increases with the discharge current, but the by-products can also be removed at the large discharge current. Hence, C/C_{in} has a maximum value at ca. 2 mA discharge current as shown in

Table 2 Material balance in removal of $(CH_3)_3N$ from N_2-O_2-H_2O

I	Inlet	Outlet					Removal*
	$(CH_3)_3N$	$(CH_3)_3N$	CH_3CHO	C_2H_5OH	$(CH_3)_2CO$	CH_3NO_2	
0.1 mA	0 ppm	ND	0.8 ppm	ND	ND	ND	
(carbon balanc	basis: 1 m³ of inlet gas)						
2.54	10^{-4} mol-C	ND	0.07×10^{-7} mol-C	ND	ND	ND	2.47×10^{-4} mol-C
(nitrogen balar	e, basis: 1 m³ of inlet gas)						
0.85	10^{-3} mol-N	ND	0	0	0	ND	0.85×10^{-3} mol-N
0.15 mA	0 ppm	ND	4.1 ppm	1.3 ppm	0.9 ppm	ND	
(carbon balanc	basis: 1 m³ of inlet gas)						
2.54	10^{-4} mol-C	ND	0.36×10^{-4} mol-C	0.11×10^{-4} mol-C	0.11×10^{-4} mol-C	ND	1.96×10^{-4} mol-C
(nitrogen balar	e, basis: 1 m³ of inlet gas)						
0.85	10^{-3} mol-N	ND	0	0	0	ND	0.85×10^{-3} mol-N
0.2 mA	0 ppm	ND	2.4 ppm	0.6 ppm	ND	ND	
(carbon balanc	basis: 1 m³ of inlet gas)						
2.54	10^{-4} mol-C	ND	0.22×10^{-4} mol-C	0.06×10^{-4} mol-C	ND	ND	2.26×10^{-4} mol-C
(nitrogen balar	e, basis: 1 m³ of inlet gas)						
0.85	10^{-3} mol-N	ND	0	0	0	ND	0.85×10^{-3} mol-N

*amount removed by deposition or particle formation
ND: not detected

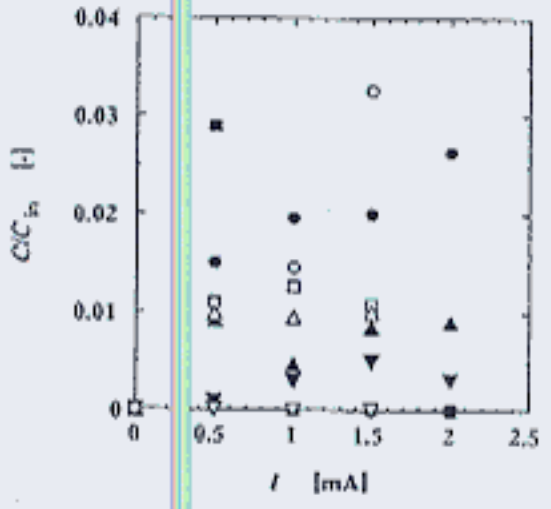

		C_{in} [ppm]	C_{H2O} [ppm]	Q [cm³/min]
○	acetald hyde	25	10000	443
△	ethanol	25	10000	443
▽	acetone	25	10000	443
□	nitrom hane	25	10000	443
●	acetald hyde	28	4950	360
▲	ethanol	28	4950	360
▼	acetone	28	4950	360
■	nitrom hane	28	4950	360

Fig. 4 Reaction b -product in removal of $(CH_3)_3N$ from N_2-H_2O

Fig. 3. One can s that the by-products can be suppressed at lower ischarge current than 0.2 mA discharge current.

2.3 Removal of $(CH_3)_3N$ from N_2-H_2O

Figure 2 sho s the influence of H_2O on the removal of $(CH_3)_3N$. One can see that 4950 ppm H_2O contributes to raising the removal efficiency of $(CH_3)_3N$. The removal efficiency of $(CH_3)_3N$ with 10,000 ppm H_2O is smaller than that with 4950 ppm H_2O because more by-products are generated as described below.

The same reaction by-products are generated in the removal of $(CH_3)_3N$ from N_2-H_2O as from N_2-O_2. Figure 4 shows the by-products with 4,950 ppm and 10,000 ppm H_2O. Compared with Fig. 3, the by-products in the removal from N_2-H_2O are much less than from N_2-O_2. This figure suggests that 10000 ppm H_2O generates more by-products than 4,950 ppm H_2O in the range of $I \geq 1$ mA and that Ψ of $(CH_3)_3N$ with 10000 ppm H_2O is smaller than that with 4,950 ppm H_2O for $I \geq 1$ mA as shown in Fig. 2.

2.4 Removal of $(CH_3)_3N$ from N_2-O_2-H_2O

Furthermore, the influence of O_2 and H_2O on the removal efficiency of $(CH_3)_3N$ has been examined. The results are shown in Fig. 5. This figure shows the removal efficiency of $(CH_3)_3N$ with 16% O_2 and 17,600 ppm H_2O. This result shows very high removal efficiency even in the low discharge current range in the presence of O_2 and H_2O.

Reaction by-products, CH_3CHO, C_2H_5OH, and $(CH_3)_2CO$, were observed. CH_3NO_2, however, was not detected. The material balance in the removal is important. Table 2 shows the carbon or nitrogen balance per 1 m³ of inlet gas of the reactor in the removal of $(CH_3)_3N$ from N_2-O_2-H_2O. It can be seen that N atom of $(CH_3)_3N$ is completely removed by deposition at the anode or particle formation. On the other hand, a part of C atom of $(CH_3)_3N$ comes out from the reactor as reaction by-products. The amount of CH_3CHO generated is larger than other compounds in the corona-discharge reactor. Since CH_3CHO is also a component of malodorous gases from crematory emission, it is im-

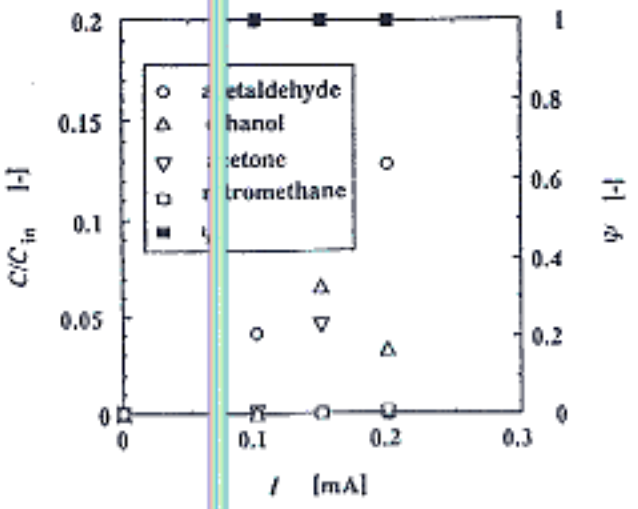

Fig. 5 Reaction by-product in removal of $(CH_3)_3N$ from N_2-O_2-H_2O (C_{in} = 19 ppm, C_{O_2} = 16%, C_{H_2O} = 17,600 ppm, Q = 410 cm³/min)

portant to decrease the amount generated. Compared with Figs. 3 and 4, one can see that the by-products can be suppressed by mixing H_2O even in the presence of O_2. Hence, when the discharge current is kept low in the presence of H_2O, it is interesting that the production of CH_3Cl can be decreased.

Conclusively, under the present experimental conditions, O_2 or H_2O enhances the removal efficiency of $(CH_3)_3N$. These results suggest that the corona-discharge reactor is applicable for the removal of $(CH_3)_3N$ from air.

2.5 TG analysis of deposit

The authors conducted removal experiments of $(CH_3)_3N$ for 5 days using the corona-discharge reactor with parallel plates as described above. The experimental conditions are shown in Table 3. Then the deposit on the anode surface was analyzed using the thermogravimetric (TG) curves were measured at 20°C/min from 20 to 1000°C.

Figure 6 shows the TG curves of the deposit formed in the removal of $(CH_3)_3N$ from N_2, N_2-O_2, and N_2-H_2O. The ordinate is the decrease of weight and the abscissa is temperature. From the TG curve of the deposit formed in the removal from N_2, the weight gradually decreases till 550°C and then a large weight loss suddenly occurs at ca. 550°C. The TG curves obtained for the removal from N_2-O_2 and N_2-H_2O suggest that the large weight loss is observed at ca. 200 or 250°C. One can see that some deposit remains even after pyrolysis at 1000°C. Hence, it can be concluded that the deposit consists of carbon compounds of high boiling point and that a part of the deposit is carbonized by pyrolysis.

The TG curve in the removal from N_2-O_2 is different from that of the deposit formed in the removal from N_2. Hence, the O_2 reaction with $(CH_3)_3N$ induces

Table 3 Experimental conditions for analysis of deposit on anode

Gas	C_{in} [ppm]	Q [cm³/min]	C_{O_2} [%]	C_{H_2O} [ppm]	I [mA]
$(CH_3)_3N$-N_2	102	251	0	0	1.0
$(CH_3)_3N$-N_2-O_2	18	411	19	0	0.1
$(CH_3)_3N$-N_2-H_2O	19	385	0	17000	0.1

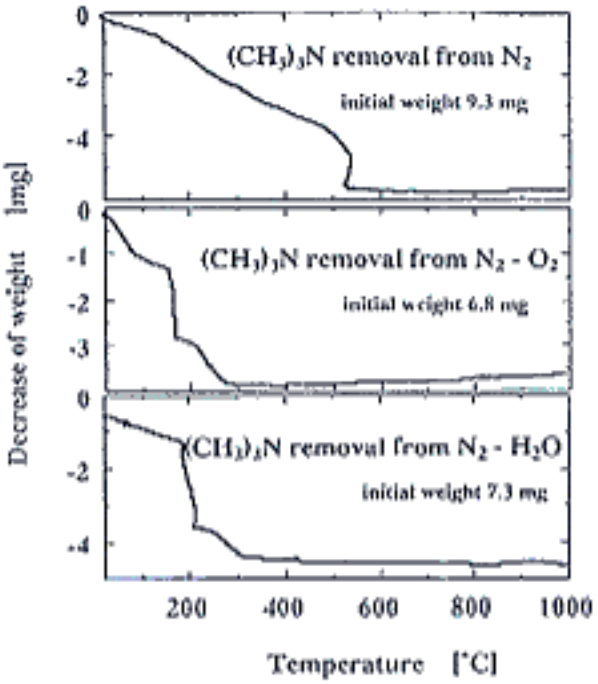

Fig. 6 TG curves of deposit formed in removal of $(CH_3)_3N$

a cyclic polycondensation producing a carbon compound. The TG analysis of the deposit formed during the removal of $(CH_3)_3N$ in N_2-H_2O suggests that the deposit is a carbon compound similar to that formed in the removal from N_2-O_2. The authors have measured O_3 concentration produced by corona discharge in N_2-H_2O mixture under the conditions of Q = 389 cm³/min, C_{H_2O} = 5600 ppm, and I = 0.1 mA. As a result, O_3 has not been generated at all. It is well known that electrons produced by corona discharge attach to H_2O, and that H^-, OH^-, O^- are produced (Massey, 1976). Hence, these ions seem to decompose $(CH_3)_3N$ and touch off a chain polycondensation reaction. Although the reaction mechanism in N_2-O_2 is different from that in N_2-H_2O, both deposits on the anode surface are similar.

The authors have found several interesting results on the formation of reaction by-products and the TG curves. The removal mechanism of $(CH_3)_3N$ cannot be explained in the present stage of investigation. Further studies should be done to elucidate the removal mechanism.

Conclusion

Trimethylamin was removed using the corona-discharge reactor. The formation of reaction by-products in the removal was discussed and the deposit at the anode of the reactor was analyzed. The following conclusions have been obtained.

(1) Although the removal efficiency of trimethylamine is low in nitrogen, the efficiency is improved greatly in the presence of oxygen or water vapor.

(2) The large amounts of reaction by-products are generated in the removal of trimethylamine from a nitrogen-oxygen mixture.

(3) Water vapor plays a role for decreasing reaction by-products formed by corona-discharge in the presence of oxygen.

(4) Trimethylamine deposits as carbon compounds of high boiling point on the anode surface by corona discharge.

Acknowledgment

This research was partially supported by Thailand Research Fund (1996–1999). The author, W. T. is grateful to the Japan Society for the Promotion of Science (JSPS) for the financial support for the visit to Kyoto University (1999).

Nomenclature

C	=	concentration	[ppm]
I	=	discharge current	[mA]
Q	=	gas flow rate	[cm³/min]
Ψ	=	removal efficiency	[−]

<Subscript>

H_2O	=	water vapor
in	=	gas inlet
O_2	=	oxygen
out	=	gas outlet

Literature Cited

Massey, S. H.; Negative Ions, Cambridge Univ. Press, London, UK (1976)

Nishida, K.; "Malodor at Cremation Facility (Part I)," *PPM*, 3, 49–58 (1988a)

Nishida, K.; "Malodor at Cremation Facility (Part II)," *PPM*, 4, 51–59 (1988b)

Nishida, K. and Y. Matsuda; "Malodor of Exhaust Gas from a Crematory," *J. Odor Control*, 10, 1–11 (1981)

Sano, N., T. Nagamoto, H. Tamon and M. Okazaki; "Removal of Iodine and Methyl Iodide in Gas by Wetted-Wall Reactor Based on Selective Electron Attachment," *J. Chem. Eng. Japan*, 29, 59–64 (1996)

Sano, N., T. Nagamoto, H. Tamon, T. Suzuki and M. Okazaki; "Removal of Methyl Iodide in Gas by Corona-Discharge Reactor," *J. Chem. Eng. Japan*, 30, 902–909 (1997a)

Sano, N., H. Tamon and M. Okazaki; "Removal of Iodine in Gas by Corona-Discharge Reactor," *J. Chem. Eng. Japan*, 30, 944–946 (1997b)

Sano, N., T. Nagamoto, H. Tamon, T. Suzuki and M. Okazaki; "Removal of Acetaldehyde and Skatole in Gas by Corona-Discharge," *Ind. Eng. Chem. Res.*, 36, 3783–3791 (1997c)

Tamon, H., H. Mizota, N. Sano, S. Schulze and M. Okazaki; "New Concept of Gas Purification by Electron Attachment," *AIChE J.*, 41, 1701–1711 (1995)

Tamon, H., N. Sano and M. Okazaki; "Influence of Oxygen and Water Vapor on Removal of Sulfur Compounds by Selective Electron Attachment," *AIChE J.*, 42, 1481–1486 (1996)

Tamon, H., H. Imanaka, N. Sano, M. Okazaki and W. Tanthapanichakoon; "Removal of Aromatic Compounds in Gas by Electron Attachment," *Ind. Eng. Chem. Res.*, 37, 2770–2774 (1998)

Tanthapanichakoon, W., P. Khuopprasarnkala, T. Charinpanitkul, H. Tamon, N. Sano and M. Okazaki; "Removal of Trimethylamine and Ammonia Using Electron Attachment Reaction," *Science Asia*, 25, 57–63 (1999)

Journal of Chemical Engineering of Japan, Vol. 34, No. 8, pp. 1012–1016, 2001 Research Paper

Reduction of NO by CO in a Pulsed Corona Reactor Incorporated with CuO Catalyst

LIWEI HUANG, TAKAAKI HARI, KATSUHIKO NAKAJYO, SHOJI OZAWA AND HITOKI MATSUDA

Research Center for Advanced Waste and Emission Management, Nagoya University, Nagoya 464-8603, Japan

Keywords: NO Reduction, CO, Nonthermal Plasma, Catalyst, CuO

Reduction of NO by CO in N_2 was experimentally investigated in a wire-in-tube pulsed corona reactor combined with CuO catalyst. The pulsed corona was produced by applying a positive pulsed high voltage (peak voltage 16–22 kV, pulse frequency 50 pps) to the wire electrode and the catalyst was coated on the surface of the aluminum film, the grounding electrode attached to the inner surface of the tube. It was demonstrated that NO could be effectively reduced to N_2 under nonthermal plasma produced by pulsed corona discharge, and the NO_2 yield was significantly suppressed with the existence of CO in the gas stream. For the pulsed corona reactor combined with CuO catalyst, the reduction of NO was 10–20% higher and NO_2 production was 50% lower than that of without catalyst in the reactor at room temperature, showing that CuO catalyst works effectively for the reduction of NO under pulsed corona discharge. A complete reduction of 500 ppm NO in a gas stream containing 1% CO was achieved at about 473 K with a pulse voltage of 18 kV in the reactor combined with CuO catalyst.

Introduction

The control of NO_x emitted from fuel combustion processes of such as diesel-fueled vehicles has become an important issue because of stringent regulations imposed on the allowable levels of NO_x emissions especially in cities. However, traditional technologies may have some problems to meet these stringent requirements. For example, the three-way catalyst for gasoline engine are unsuitable for diesel engine, because the exhaust gas from diesel engine contains high concentrations of O_2, much particulate matter and SO_2 (Farrauto and Heck, 1999). Therefore, new techniques based on nonthermal plasma for the abatement of NO_x emissions from fuel combustion processes have been received much attention in recent years, because of nonthermal plasma has unique characteristics in molecule dissociation and chemical reaction-promoting (Penetrante *et al.*, 1995; Urashima *et al.*, 1998; Yamamoto, 2000).

Generally, nitrogen oxide accounts for most of NO_x discharged from combustion processes. The mechanism for NO removal under nonthermal plasma is regarded to proceed both reduction and oxidation processes (Gentile and Kushner, 1995; Sathiamoorthy *et al.*, 1999). It has been ascertained that NO reduction proceeds mainly via a fast reaction (1) (Behbahani *et al.*, 1982; Harano *et al.*, 1998).

$$N + NO \rightarrow N_2 + O \qquad K = 3.1 \times 10^{-11}\ [cm^3 \cdot s^{-1}] \quad (1)$$

The N atom in this reaction is produced mainly from dissociation of N_2 molecule by energetic electron impact. The oxidation of NO to NO_2 is attributed to the reactions (2) and (3).

$$O + NO + M \rightarrow NO_2 + M \qquad K = 9.1 \times 10^{-32} T^{-1.6}\ [cm^6 \cdot s^{-1}] \quad (2)$$

$$O_3 + NO \rightarrow NO_2 + O_2 \qquad K = 2.0 \times 10^{-12} \exp(-1400/T)\ [cm^3 \cdot s^{-1}] \quad (3)$$

It is thought that the reduction of NO to N_2 is more difficult than the oxidation of NO to NO_2, because much higher electron energy is required to promote the reduction reaction efficiently. Therefore, the oxidative removal of NO by means of nonthermal plasmas attracted most previous researches. However, in such a practical application as automobile exhaust gas treatment, reducing NO to N_2 is more attracting than oxidizing NO to NO_2, because no additional processes like scrubbing systems are needed for further NO_2 treatment.

In this study, the reduction of NO to N_2 by CO which is also a pollutant gas contained in exhaust gases

Received on December 21, 2000. Correspondence concerning this article should be addressed to L. Huang (E-mail address: hlw@reseve.nagoya-u.ac.jp).
Partly presented at The 33rd Autumn Meeting of The Society of Chemical Engineers, Japan.

Advanced Powder Technol., Vol. 12, No. 2, pp. 265–268 (2001)

News bulletin

How does APT2000 impact particle technology in Thailand — let me count the ways

WIWUT TANTHAPANICHAKOON

The Powder Technology Center, Faculty of Engineering, Chulalongkorn University, Bangkok 10330, Thailand

Received 15 January 2001; accepted 31 January 2001

Before starting to count the ways, I wish to give a brief introduction to the roles of the lesser-known players and some historical background.

1. WHAT IS APT2000?

It is the First Asian Particle Technology Symposium co-organized during 13–15 December 2000 in Bangkok by the Thai Powder Technology Center (TPTC) of Chulalongkorn University (CU) and The Society of Powder Technology, Japan (SPTJ) with strong support from the Association of Powder Process Industry and Engineering (APPIE), Japan, and cooperation from numerous societies and associations in Asia and Oceania. Please refer to the web site [http://www.apt2000.org] for more details.

2. WHY BANGKOK? WHY NOT TOKYO OR ELSEWHERE?

Located near the geographical center of Asia, Bangkok is conveniently and economically accessible by air. The 'City of Angels' or 'Krungthep' — the official Thai name of Bangkok — offers diverse cultural settings, renowned Thai-style hospitality, niche and popular restaurants offering Thai and cosmopolitan cuisines, vast shopping malls and complexes, as well as numerous tourist landmarks, such as magnificent temples, majestic palaces — all at very reasonable prices in comparison with Japan. If these reasons are not good enough, how about adding fascinating entertainment venues and night life for the more venturous souls? To TPTC and SPTJ, however, one of the important reasons is that the year 2000 coincides not only with

the dawn of a new millennium — an auspicious moment to start a new venture — but also the 10th anniversary of TPTC.

Compared to SPTJ and APPIE, TPTC is like a primary school graduate, although it is more firmly established than similar organizations in other Asian countries with the exception of China, South Korea, Russia and Taiwan. As described in the *Millennial Edition on Particle Technology*, published by TPTC in December 2000, TPTC owes its inception and subsequent success to the strong support rendered by APPIE, SPTJ, CU as well as numerous individuals in both countries.

3. WHAT HAS TPTC CONTRIBUTED TO PARTICLE TECHNOLOGY (PT) IN THAILAND DURING ITS FIRST DECADE?

Definitely a lot. If interested, please contact the author for a copy of TPTC *Millennial Issue*, which is bilingual in Thai and English.

4. BACKGROUND OF APT2000

First conceived in 1997 — a year before the World Congresss on Particle Technology in Brighton in 1998 — the formal kick-off for APT2000 was symbolized by the establishment of its International Organizing Committee (IOC) during 13–15 December 1998 at the Mandarin Hotel, Bangkok — exactly the same month, days and venue as the real APT2000.

5. HOW DOES APT2000 IMPACT PT IN THAILAND?

Now let me count the ways APT2000 has impacted on particle technology in Thailand (and more or less in the whole of Asia).

- First-ever APT, the birth of a regular series of symposia to be held biannually in Asia.
- First exhibition (panels/catalogs) aimed solely at PT in Thailand.
- The largest gathering (297 persons) of particle technologists and scientists (PTS) at any symposium/conference in Thailand.
- The largest number (251 persons) of non-resident PTS's at a single gathering in Thailand.
- The largest number of participating countries (20 countries) in a PT event in Thailand: 14 from Asia–Oceania (Australia, China, Indonesia, India, Japan, Malaysia, Mongolia, Philippines, Russia, Singapore, South Korea, Taiwan, Thailand, Vietnam) as well as France, Mexico, Netherlands, Sweden, UK and USA.
- The highest number of PT research papers submitted (231) and presented any symposium/conference in Thailand.

- The ighest number of plenary, invited lectures and technical seminars on PT in any ymposium/conference in Thailand.
- A sp cial Asian Complex event designed to provide the latest live information on p wder-related business and technology presented by the Chairman of Thai Fede ation of Industries (Mr Tawee Butsuntorn) and the representatives of IOC cour ries.
- The ighest print run on PT published by TPTC (3,000 copies of TPTC Millennial dition).
- The rgest number of foreign visitors to the TPTC Lab in CU in a single day (abo t 70 persons).
- Num rous contacts with TPTC from industrial companies after the conclusion of APT 000 (for technical consultation and testing services).
- Num rous inquiries from industrial companies and manufacturers about similar futu events in Thailand.
- The ounding Director of TPTC becoming the current President of CU, who presi ed over the Opening Ceremony of APT2000.
- The ulmination of APPIE's and SPTJ's decade-long support to TPTC which has beco e a key player in the promotion and development of PT in Thailand.

It ha been decided that the Second APT will be held in Malaysia in 2003 instead of 2002 in order to avoid unfavorable impact on the World Congress on Particle Technology 2002 in Sydney. In addition, as an important by-product of TPTC's remarkable success, APPIE has decided to assist the establishment of a second Powder Technology Center in a suitable Asian country in the near future. Undoubtedly there are several more ways, both direct and indirect, that APT2000 has impacted, and will continue to impact, on the development of PT and related industries in Thailand, but I am too tired now to continue counting.

6. MY PERSONAL INVOLVEMENT WITH PT

It goes without saying that particle science and technology has long had, and will continue to have, a significant impact on the development of Thai industries and society, as well as my own academic and research career. Though I am said to be the first Thai Chemical Engineering graduate who received his BEng in Japan (Kyoto University), I did not do any research in PT while in Kyoto as a Monbusho Scholarship student nor during my graduate study in the University of Texas at Austin. In fact, I studied in Dr Ryozo Toei's Lab and my senior thesis advisor was Dr Morio Okazaki, though I did study *Process Control* with Dr Koichi Iinoya. So I knew only a little about PT when I met Dr Kanji Matsumoto at the First Thailand–Japan Joint Seminar on Powder Technology in Bangkok more than 10 years ago. I suppose the reason Professor Iinoya has given me strong support

in he establishment and running of TPTC and the Thai Assosciation for Particle In itute is that he believed I could do it and not for personal gains. Thanks in part to ny Japanese language fluency and educational background, I am 'fortunate' to ha e received many helping hands from a huge number of individuals, including M Osamu Doi, Mr Tsunemi Hayashi, Dr K. Matsumoto and Dr Chikao Kanaoka, ju to mention a very few, as well as the member companies of APPIE's TPTC C peration Committee (TPTCCC) and subsequently Thai Subcommittee. On th Thai side, many PT colleagues and TPTC members, including Dr Sirikalaya Su achittanon, Dr Tawatchai Charinpanitkul, Dr Hathaichanok, Duriyabunleng, M Nattaporn Tonanon and Mr Preecha Sangtherapitikul, have contributed to the su cess of TPTC and APT2000.

7. ONCLUSION

A ording to the feedback and comments I have received from many participants, A T2000 was well organized and had more impact than originally expected. Thus I v sh to take this opportunity to sincerely thank all persons and organizations men- tio ed above, as well as the IOC (headed by Dr M. Senna), the International Advi- so Board, the Scientific and Technical Committee (headed by Dr Y. Fukumori), th Local Organizing Committee, and the numerous individuals, staff and students wh worked behind the scene for the great success of APT2000. Last, but not le t, I want to thank all the participants, especially non-residents, who really made A T2000 a fruitful and rewarding event. I am convinced that the true impact of A T2000 on Thailand and other Asian countries will have long-lasting effects and no only short-term ones.

et us meet at the next APT2003 in Malaysia.

エアロゾル研究，16（1），68（2001）

The First Asian Particle Technology Symposium 2000 (APT2000)

Wiwut TANTHAPANICHAKOON*
and Tawatchai CHARINPANITKUL*

2000年12月13～15日まで，タイ・バンコクのMandarin Hotelで The First Asian Particle Technology Symposium, APT2000が開催されました。このシンポジウムは，20世紀に別れを告げ新しい21世紀の到来を視うと同時に，アジア諸国，そしてヨーロッパ，アメリカ，オーストラリアの粉体工学研究者を一堂に集める場として企画されました。このようにたいへん意義のあるシンポジウムの第1回を主催できたことは，われわれThai Powder Technology Center（TPTC）にとって，大きな光栄でした。

APT2000の参加者数は合計297名で，その内249名（約84%）がタイ以外の国からの参加者でした。大学からの参加者は21名，企業からの参加者は79名で，大学からの参加者の内46名は学生でした。国別で参加者をみると，オーストラリア（9），中国（7），フランス（2），インド（1），インドネシア（2），日本（132），マレーシア（4），モンゴル（2），オランダ（1），フィリピン（2），シンガポール（1），韓国（48），スウェーデン（1），台湾（8），英国（3），アメリカ合衆国（2），ベトナム（7）でした。32のセッションで発表された論文は156件あり，全体講演は13件ありました。シンポジウムの会場はやや小さかったかもしれませんが，各セッションで活発な議論が行われました。

発表された研究内容は，基礎（たとえば粒子のキャラクタリゼーション，粒子生成など）から応用（薬剤，環境，生体影響など）まで非常に広い分野を網羅していました。発表された研究成果は，タイ国だけでなくアジア諸国また世界にとって役に立つと信じております。とにかく，大きな可能性を持つ粉体工学・エアロゾル工学の今後の発展は，タイの研究者や学生などに大きい影響を与えるのは間違いありません。

今回のAPT2000は研究発表のセッションだけでなく，さまざまな参加者の要求に応えるために，セミナーと展示会，見学会等の催しが加えられました。その中の一つにアジア特別複合プログラム（Asian Special Complex）がありました。このプログラムでは，各国の粉体工学研究の現状，学会と産業界との協力体制等について報告がありました。

オープニング・セレモニー（神戸学院大学・福森先生御提供）

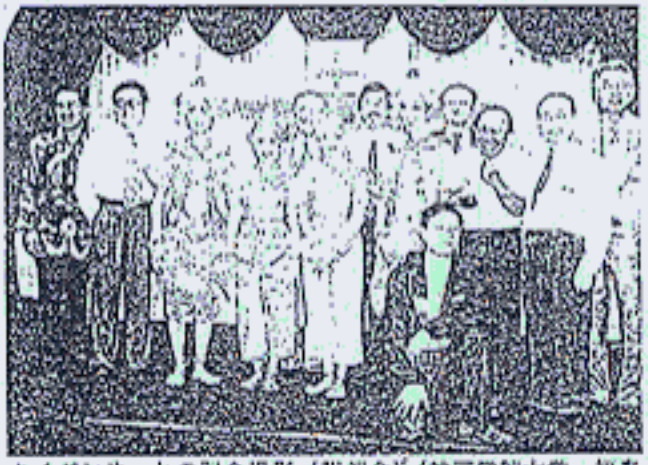
タイダンサーとの記念撮影（懇親会）（神戸学院大学・福森先生御提供）

多くの方々のご支援によりAPT2000は成功裏に閉会し，その成果は思った以上のものがありました。次のシンポジウムAPT2003はMalaysiaで開かれることが，本シンポジウムの期間中に決定されました。第2回APTにおいても，粉体工学，エアロゾル工学に関わっている方々により，新しい研究成果の発表や活発な議論が積極的に行われ，すばらしいシンポジウムができるよう期待したいと思います。

* Department of Chemical Engineering, Faculty of Engineering, Chulalongkorn University
Phyathai Rd., Patumwan, Bangkok 10330, Thailand

ELSEVIER

Chemical Engineering Journal 86 (2002) 11–15

Chemical Engineering Journal

www.elsevier.com/locate/cej

New s mple mathematical model of a honeycomb rotary absorption-type dehumidifier

Wiwut Tanthapanichakoon*, Anawut Prawarnpit

Faculty of Engine ing, Department of Chemical Engineering, Chulalongkorn University, Patumwan, Bangkok 10330, Thailand

.bstract

A simplified mathematica model consisting of ordinary differential equations has been proposed and found to accurately predict the ynamic performance of a h eycomb rotary absorption-type dehumidifier in a beverage factory. The model was validated experimentally sing the transient measure ent data on the air properties at the outlets of both the dehumidification and regeneration sections. Good greement between the pred ted and recorded data at each time has been observed. The model is numerically stable and easy to simulate.

Keywords: Rotary dehumidifier; oneycomb; Lithium chloride salt; Solid absorbent; Dynamic model

1. Introduction

For hygienic reasons th equipment as well as the floor pace in the concentrate p paration room of a modern bev- rage factory are daily cle ed, scrubbed, mopped and left to dry-out overnight. To deh nidify the circulating humid air nd ensure the dry-out of th wet floor in the closed room, the resent factory employs tw identical continuous rotary de- umidifiers. In contrast to sorption-type dehumidifiers that se silica gel, molecular s ve, etc. as adsorbent, the tested sorption-type dehumidif r uses a lithium chloride-coated neycomb. As the rotor lowly turns, humid room air is rculated through and de midified in the absorption sec- n of the honeycomb. eantime ambient air is heated about 350 K and sim taneously sent counter-current rough the regeneration ection to dry the moist solid sorbent.

In the past all invest ations have focussed on the lsorption-type rotary deh midifier and there are no publi- tions on the rotary abso tion type. Kodama et al. [1–3] xperimentally investigate the temperature effect and op- mal operation of a therm -swing honeycomb rotor adsor- er. To predict simultane s heat and mass performance f the regenerator of a rot y dehumidifier, Maclaine-cross nd Banks [4] and Banks [,6] utilized linear and nonlinear nalogy method, whereas Mathiprakasam and Lavan [7] redicted the performance f adiabatic desiccant dehumidi- ers using linear solutions. These earlier methods are handy but not so rigorous and did not provide detailed or transient information.

To numerically solve the governing partial differential equations of a rotary adsorption-type dehumidifier, Holmberg [8], Jurinak and Mitchell [9] and Schultz and Mitchell [10] developed and applied an explicit-finite difference technique. To ensure unconditional numerical stability and reduce computational time, Zh ng and Worek [11] proposed and applied an implicit-finit difference technique for the numerical simulation.

In contrast the authors h ve developed a new, simple dynamic model for the honeycomb rotary dehumidifier consisting of a set of nonlinear ordinary differential equations. The validity of the present model was substantiated by comparing the simulated results with the transient experimental values. The model accuracy with respect to the key variables (outlet and inlet air temperatures and humidities) is better than ±2%.

2. Mathematical model of rotary dehumidifier

A typical honeycomb rotor consists of thousands of almost identical narrow straight slots uniformly distributed over its rotor cross-section as shown in Fig. 1. Because of geometric similarity, the multiple annular layers of straight slots in the dehumidification and the regeneration sections can be represented by a "representative annulus" of thickness Δr equaling one slot height. In this way, the three cylindrical coordinates (r, θ, z), say radial, angular and axial directions,

* Corresponding author. Fax: + 5-2-218-6894.
-mail address: twiwut@chula.a h (W. Tanthapanichakoon).

385-8947/02/$ – see front matt
I: S1385-8947(01)00266-

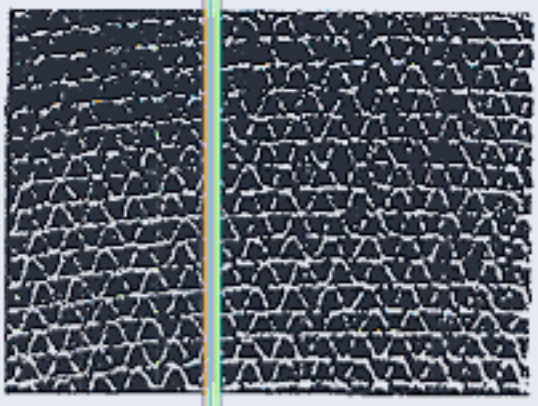

Fig. 1. oneycomb structure.

spectively, in the m del can rationally be reduced to ate two coordinates (θ z). By taking into account each constituent slot within he total M identical slots in the θ-direction spanning th entire cross-section of the representative annulus, the maining space variable is z. For example, $M = 400$ wit the first 100 slots being the regeneration section. Of cour , a second independent variable in the model is the time t. n other words, the dynamic behavior of the honeycomb r tor can be simulated by following the transient changes curring in the z-direction within each of the M slots as t rotor slowly turns.

The following simpli ing assumptions are made:

1. Air flow is uniforml distributed across the dehumidification and the regen ation cross-sections.
2. The air stream flowir through each slot is assumed to be plug or piston flow. I the plug flow model, variation does not exist in the radial direction but exists only in the axial or z-direction. Theo tically and conceptually, the plug flow model has been hown to be equivalent to the model of a series of equal-v lume CSTRs in which an infinitely large number of com ietely mixed cells, each of infinitely small thickness, are nnected in series. For practical reasons, the plug flow odel of each slot will be approximated by an equivale CSTR model consisting of N cells in series as shown in Fig. 2, N being 10, 20 or more [12].
3. Gas-phase heat conduction and mass diffusion in the axial direction are negligibly small compared to the convective effects in the same slot.
4. Each slot is adiabatic and heat conduction along the slot wall may be neglected.
5. Interphase moisture transfer between the gas and solid absorbent phases in the slot is controlled by gas-phase film resistance since the absorbent layer is essentially non-porous.
6. Heat of absorption of the moisture can be approximated by the latent heat of vaporization of water.

For slot no. j of the regeneration section ($j = 1, 2, \ldots, M_r$), the unsteady mass and energy balances for cell no. i ($i = 1, 2, \ldots, N$) are as follows:

Gas-phase moisture balance:

$$\frac{\mathrm{d}(H_i)}{\mathrm{d}t} = \frac{NG_{\mathrm{Fa}}V_{\mathrm{Hi}}}{L}(H_{i-1} - H_i) - \frac{kA_{\mathrm{h}}NV_{\mathrm{Hi}}}{\varepsilon LA_{\mathrm{c}}}(H_i - H_{\mathrm{Si}}) + \left(\frac{H_i}{V_{\mathrm{Hi}}}\right)\frac{\mathrm{d}(V_{\mathrm{Hi}})}{\mathrm{d}t} \quad (1)$$

where H_i and H_{Si} are the humidity and saturated humidity of hot air in cell no. i, respectively ($\mathrm{kg_{water\ vapor}\ kg_{dry\ air}^{-1}}$), V_{Hi} the specific volume of humid air ($\mathrm{m^3\ kg_{dry\ air}^{-1}}$), G_{Fa} the mass flow rate of humid air ($\mathrm{kg_{dry\ air}\ m^{-2}\ s^{-1}}$), t the time (s), L the length of each rotor slot, N represents the number of cells in each slot, k the mass transfer coefficient between moist material and hot air ($\mathrm{kg\ m^{-2}\ s^{-1}}$), ε the honeycomb porosity (–), A_{h} the internal surface area of each cell ($\mathrm{m^2}$), A_{c} the total cross-sectional area of each cell ($\mathrm{m^2}$). The Ranz–Marshall correlation is used to estimate the value of k [13].

Solid-phase moisture balance:

$$\frac{\mathrm{d}(W_i)}{\mathrm{d}t} = k(H_i - H_{\mathrm{Si}})\frac{NA_{\mathrm{h}}}{LA_{\mathrm{c}}\rho_{\mathrm{SB}}} \quad (2)$$

where W_i is the moisture in the absorbent material in cell i ($\mathrm{kg_{water}\ kg_{dry\ material}^{-1}}$), ρ_{SB} the apparent density of dry absorbent material in the rotor ($\mathrm{kg\ m^{-3}}$).

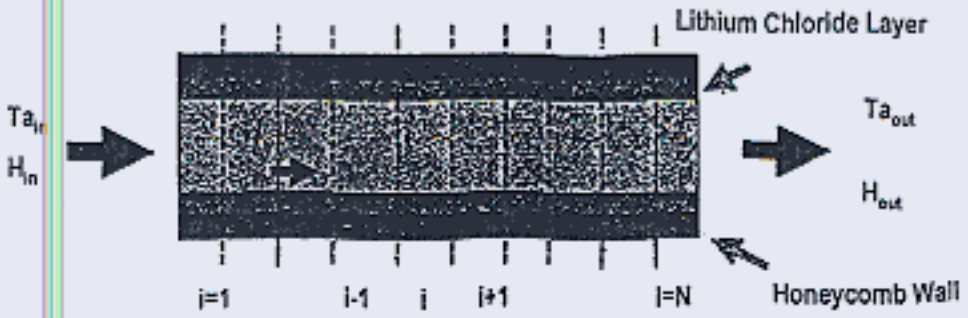

Fig. 2. Representation of a typical honeycomb slot as a series of completely mixed cells.

Gas-phase energy b ance:

$$\left(\frac{C_{pA}+C_{pv}H_i}{V_{Hi}}\right)\frac{d(T_{Ai})}{d}$$
$$=\frac{NG_{Fa}}{L}(C_{pA}+C_{p}H_{i-1})(T_{A(i-1)}-T_{Ai})$$
$$-\frac{h_c N A_h}{\varepsilon A_c L}(T_{Ai}-T_{i})+\left(\frac{kA_hN}{\varepsilon LA_c}\right)(H_i-H_{Si})$$
$$\times(C_{pw}T_{Si}+C_{pv}T_{Ai}-T_{Si}))+\left(\frac{C_{pA}T_{Ai}}{V_{Hi}^2}\right)\frac{d(V_{Hi})}{dt} \quad (3)$$

where C_{pA}, C_{pv}, C_{pw} re the specific heat of dry air, water vapor and liquid water respectively (kJ kg^{-1} K^{-1}), T_{Ai} and T_{Si} are the temperature of humid air and solid absorbent in cell no. i, respectively K), h_c the heat transfer coefficient between the gas- and s lid-phase (kJ m^{-2} s^{-1}).

Solid-phase energy b lance:

$$(\rho_{FB}C_{pFB}+\rho_{SB}C_{pSB}+\rho_{SB}C_{pw}W_i)\frac{d(T_{Si})}{dt}$$
$$=\left(\frac{kA_hN}{LA_c}\right)(H_i-H_{Si})(\lambda_{Si}-C_{pw}T_{Si})$$
$$+\frac{h_cA_hN}{LA_c}(T_{Ai}-T_{Si}) \quad (4)$$

where λ_{Si} is the latent eat of vaporization at temperature T_{Si} in cell no. i (kJ kg$_{der}^{-1}$), ρ_{FB} the apparent density of honeycomb wall (kg m^{-3}).

It should be noted t at a similar set of equations is applicable to the slots in the dehumidification section (j = 101, 102, ..., 400), ex ept that the air flow direction is reversed.

Air circulation duri the night inside the closed room can be approximated a a series of R imaginary completely mixed compartments (= 2–4). Here R is the number of compartments in the r om. As dehumidified air circulates through the room, it pic s up moisture from the wet concrete floor thus gradually dr ng out the floor. Because of space limitation the model eq itions for the room are omitted here. The fourth order Rung -Kutta method is used to integrate the set of four (MN + R) ordinary differential equations simultaneously. By ch osing the time step of integration appropriately, at the en of each time step, slot no. j will rotate to replace the no slot $j+1$ successively in circle. Similarly, slot no. M w l replace slot no. 1 after each time step.

3. Experimental

The tested honeycon rotor [14] has a 52.5 cm diameter and 10 cm width. F 3 shows a schematic diagram of the honeycomb rotor humidifier. The area ratio of the dehumidification to th regeneration section is 3:1. The

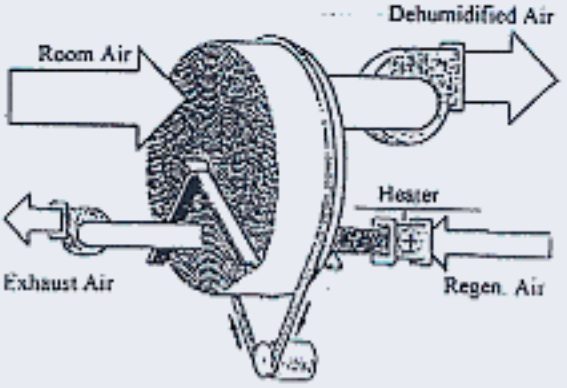

Fig. 3. Schematic diagram of honeycomb rotor dehumidifier.

rotary dehumidifier is operated overnight in a closed room with 45 m^2 floor area. Temperature of the heat ambient air entering the regeneration section is set constant at 350 K. Wet- and dry-bulb temperatures of the ambient air (before the air heater) of room and dehumidified air at the outlet of the absorption section were recorded continuously. The air

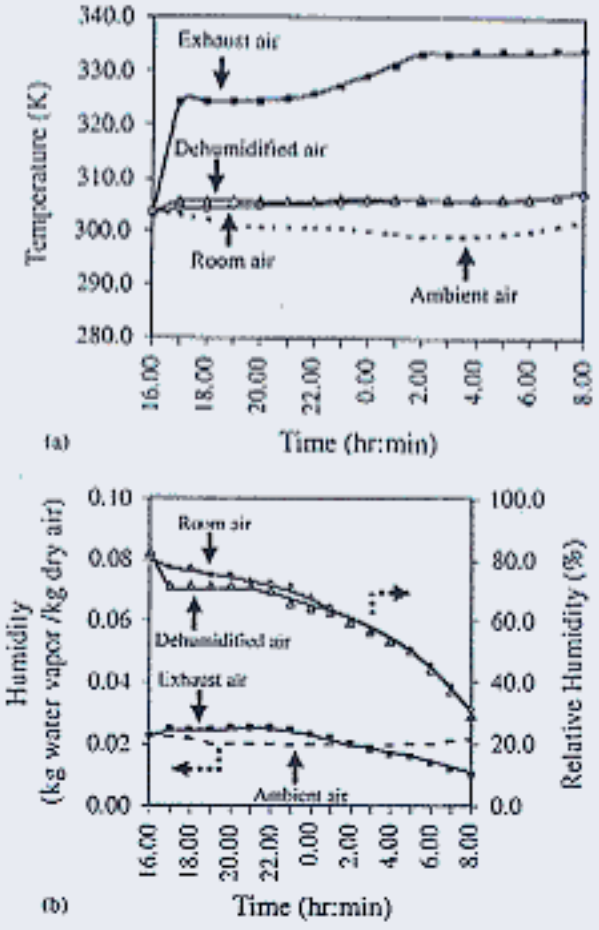

Fig. 4. (a) Comparison of the predicted air temperatures with the experimental results (T_{regen} = 353 K, $v_{abs,in}$ = 1.37 m/s, $v_{regen,in}$ = 1.01 m/s, rotational speed = 10 rph); (b) comparison of the predicted air and relative humidities with the experimental results (T_{regen} = 353 K, $v_{abs,in}$ = 1.37 m/s, $v_{regen,in}$ = 1.01 m/s, rotational speed = 10 rph).

flow rates across the ab rption and regeneration sections are 22 and 5.4 m^3/s, resp ctively.

4. Results and discussi n

The observed ambien air conditions are used as time-dependent inputs to the eater of the regeneration section. Since the room is compl tely closed off at night, only the initial conditions in the r om at the start of operation of the rotary dehumidifier are needed to run the simulation. Fig. 4 shows a typical example of the ambient air (broken line) and the simulated (solid line) vs. experimental values (dots) of the various air temperatures and humidities. Evidently the predicted and observed values of the dehumidified (absorption outlet), room and exhaust air (regeneration outlet) are in very good agreement. Though not shown here, additional tests carried out on several other days

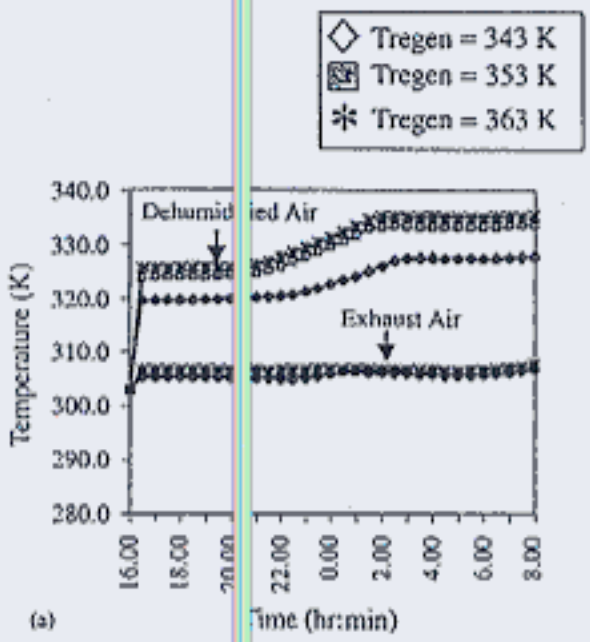

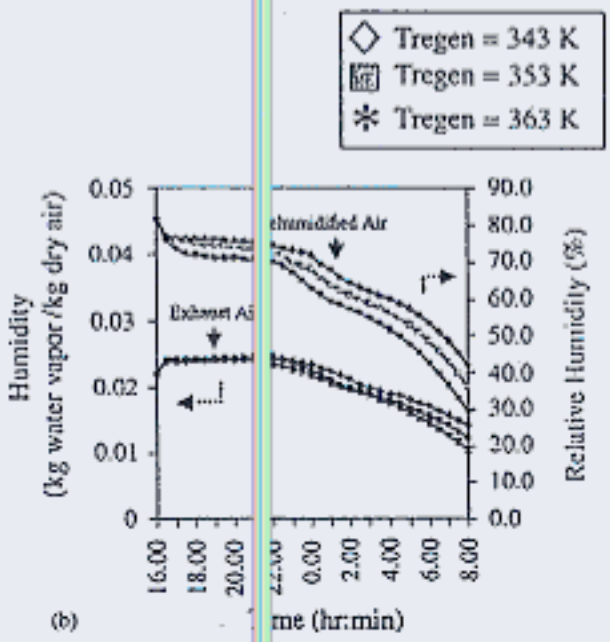

Fig. 5. (a) Comparison of th predicted air temperatures at various regenerated temperatures ($v_{abs.}$ = 1.37 m/s, $v_{regen.in}$ = 1.01 m/s, rotational speed = 10 rph); (b) comparison of the predicted air and relative humidities at various regenerated temperatures ($v_{abs,in}$ = 1.37 m/s, $v_{regen.in}$ = 1.01 m/s, rotational speed = 10 rph).

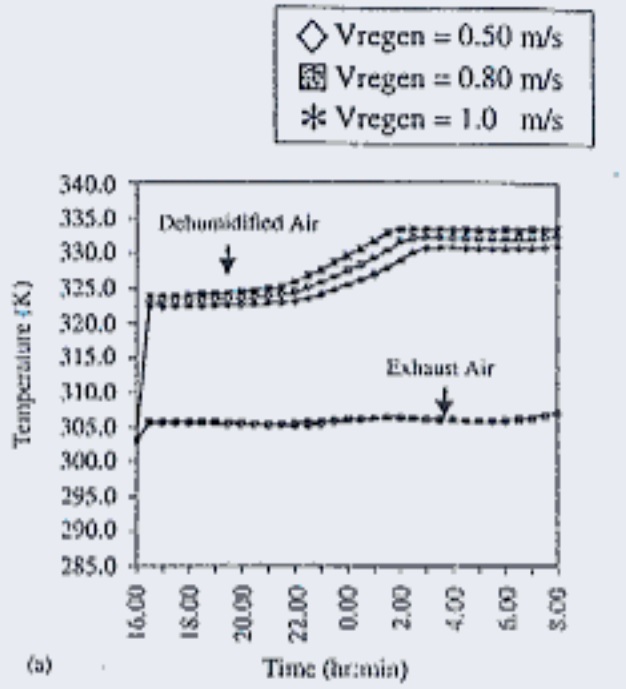

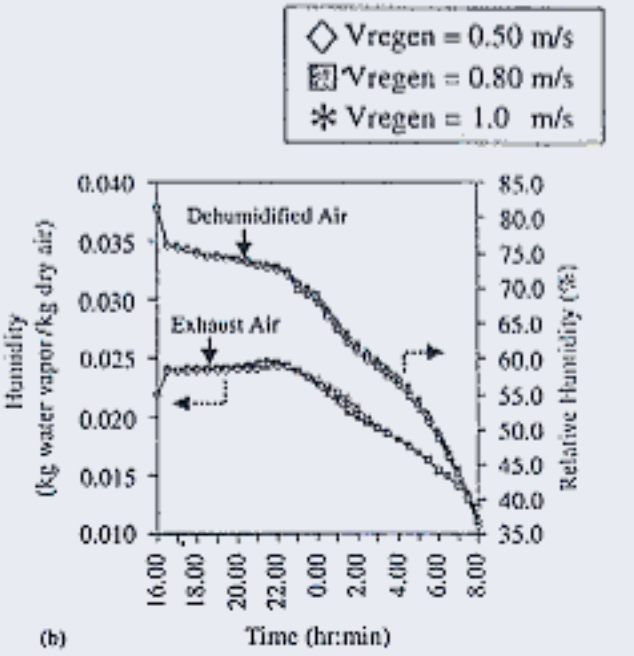

Fig. 6. (a) Comparison of the predicted air temperatures at various regenerated velocities (T_{regen} = 353 K, $v_{abs,in}$ = 1.37 m/s, rotational speed = 10 rph); (b) comparison of the predicted air and relative humidities at various regenerated velocities (T_{regen} = 353 K, $v_{abs,in}$ = 1.37 m/s, rotational speed = 10 rph).

also gave the same g d agreement. Thus it may be concluded that a simple ynamic model for the honeycomb rotary dehumidifier h successfully been developed and validated.

Next the effects of he regenerator's inlet air temperature and velocity on t efficiency of dehumidification are investigated. As shown n Fig. 5, the temperature and humidity of both the dehumi ified and exhaust air depend significantly on the regenera r's inlet air temperature. Obviously, the humidity of room ir can be reduced faster at a higher regenerator's tempera re. The effect of the regenerator's air velocity is shown Fig. 6. It can be seen that the air velocity has insignific t influence on the dehumidification efficiency.

5. Conclusion

The new simple ynamic model has been shown to simulate the dynamic performance of a honeycomb rotary dehumidifier that ag es well with experimental results. Though the model as developed and validated for an absorption-type dehu idifier, the approach should also be applicable to the adso tion-type dehumidifier. Coupled with a simple model for th humid air in a closed room with wet floor, the present mo l has also proved successful in predicting the property c ange in the room air and the decreasing amount of water maining on the wet concrete floor. In the next investigatio the coupled models will be used to obtain an optimal set f operating conditions that minimizes the energy and/or ti e required to dry-out the wet floor overnight.

Acknowledgements

Financial support from Thailand Research Fund (Senior Research Scholar Program) for WT is gratefully acknowledged. Preparation of the manuscript is aided by Ornjira Rungarunsangchai who also received partial financial support from the same TRF Program.

References

[1] A. Kodama, M. Goto, T. Hirose, T. Kuma, J. Chem. Eng. Jpn. 26 (1993) 530–535.
[2] A. Kodama, M. Goto, T. Hirose, T. Kuma, J. Chem. Eng. Jpn. 27 (1994) 644–649.
[3] A. Kodama, M. Goto, T. Hirose, T. Kuma, J. Chem. Eng. Jpn. 28 (1995) 19–24.
[4] I.L. Maclaine-cross, P.J. Banks, Int. J. Heat Mass Transfer 15 (6) (1972) 1225–1242.
[5] P.J. Banks, ASME J. Heat Transfer 107 (1985) 222–229.
[6] P.J. Banks, ASME J. Heat Transfer 107 (1985) 230–238.
[7] B. Mathiprakasam, Z. Lavan, ASME J. Solar Energy Eng. 102 (1980) 73–79.
[8] R.B. Holmberg, ASME J. Heat Transfer 101 (1979) 205–210.
[9] J.J. Jurinak, J.W. Mitchell, J. Heat Transfer Trans. ASME 106 (1984) 638–645.
[10] K.J. Schultz, J.W. Mitchell, ASME J. Solar Energy Eng. 111 (1989) 286–291.
[11] W. Zheng, W.M. Worek, Numer. Heat Transfer A 23 (1993) 211–232.
[12] D.M. Himmelblau, K.B. Bischoff, Process Analysis and Simulation, Wiley, New York, 1970.
[13] J.H. Perry, Chemical Engineers' Handbook, 3rd Edition, McGraw-Hill, New York, 1958.
[14] A. Prawarnpit, Simulation of rotary adsorption dehumidifier system, M.S. Thesis, Department of Chemical Engineering, Chulalongkorn University, Bangkok, Thailand, 1999.

รายชื่อผู้ทำงานในโครงการ

ชื่อ - นามสกุล	ตำแหน่งวิชาการ		ต้นสังกัด	ตำแหน่งในโครงการ	สถานภาพปัจจุบัน
	เมื่อเข้าร่วมโครงการ	ปัจจุบัน			
1) ท.ดร. วรพล ตันตะพานิชกุล	ผู้ช่วยศาสตราจารย์	ผู้ช่วยศาสตราจารย์	จุฬาลงกรณ์มหาวิทยาลัย	นักวิจัย	ผู้ช่วยศาสตราจารย์
2) รศ.ดร. ศิริกัลยา สุวจิตตานนท์	รองศาสตราจารย์	รองศาสตราจารย์	มหาวิทยาลัยเกษตรศาสตร์	นักวิจัย	รองศาสตราจารย์
3) รศ.ดร. ธวัชชัย ชรินพาณิชกุล	ผู้ช่วยศาสตราจารย์	รองศาสตราจารย์	จุฬาลงกรณ์มหาวิทยาลัย	นักวิจัย	รองศาสตราจารย์
4) อ.ดร. เจิดศักดิ์ ไชยคุนา	อาจารย์	อาจารย์	จุฬาลงกรณ์มหาวิทยาลัย	นักวิจัย	อาจารย์
5) อ.ดร. เดชา ฉัตรศิริเวช	อาจารย์	ผู้ช่วยศาสตราจารย์	จุฬาลงกรณ์มหาวิทยาลัย	นักวิจัย	ผู้ช่วยศาสตราจารย์
6) อ.ดร. สมประสงค์ ศรีชัย	อาจารย์	ผู้ช่วยศาสตราจารย์	จุฬาลงกรณ์มหาวิทยาลัย	นักวิจัย	ทำงานเอกชน
7) ผศ.ดร.หทัยชนก ดุริยะบรรเลง	ผู้ช่วยศาสตราจารย์	รองศาสตราจารย์	จุฬาลงกรณ์มหาวิทยาลัย	นักวิจัย	รองศาสตราจารย์
8) อ.ดร.ศราวุธ ริมดุสิต	อาจารย์	อาจารย์	จุฬาลงกรณ์มหาวิทยาลัย	นักวิจัย	อาจารย์
9) อ.ณัฐพร ไทฌานนท์	อาจารย์	อาจารย์	จุฬาลงกรณ์มหาวิทยาลัย	นักวิจัย	อาจารย์
10) นายจิระศักดิ์ แสงพุ่ม	นักศึกษา	จบการศึกษา	จุฬาลงกรณ์มหาวิทยาลัย	นักศึกษาปริญญาเอก	จบการศึกษา
11) นายกิตติศักดิ์ ลาภสุริยกุล	นักศึกษา	จบการศึกษา	จุฬาลงกรณ์มหาวิทยาลัย	นักศึกษาปริญญาโท	จบการศึกษา
12). นายเศรษฐา ตันติโรจนาเมธ	นักศึกษา	จบการศึกษา	จุฬาลงกรณ์มหาวิทยาลัย	นักศึกษาปริญญาโท	จบการศึกษา
13). นายอุดมเดช อาสิงสมาณัฐ์	นักศึกษา	จบการศึกษา	มหาวิทยาลัยเกษตรศาสตร์	นักศึกษาปริญญาโท	จบการศึกษา
14) นายจิตติวุฒิ เพชรมุนี	นักศึกษา	จบการศึกษา	จุฬาลงกรณ์มหาวิทยาลัย	นักศึกษาปริญญาโท	จบการศึกษา
15) นายจักรกฤษณ์ แย้มเกตุ	นักศึกษา	จบการศึกษา	จุฬาลงกรณ์มหาวิทยาลัย	นักศึกษาปริญญาโท	จบการศึกษา
16) นายพิเชฐ อินทร์เอื้อ	นักศึกษา	จบการศึกษา	จุฬาลงกรณ์มหาวิทยาลัย	นักศึกษาปริญญาโท	จบการศึกษา

ชื่อ - นามสกุล	ตำแหน่งวิชาการ		ต้นสังกัด	ตำแหน่งในโครงการ	สถานภาพปัจจุบัน
	เมื่อเข้าร่วมโครงการ	ปัจจุบัน			
17) นายกิตติพงษ์ พัฒนทอง	นักศึกษา	จบการศึกษา	จุฬาลงกรณ์มหาวิทยาลัย	นักศึกษาปริญญาโท	จบการศึกษา
18) น.ส.อรัญญา ทองเขี่ยว	นักศึกษา	จบการศึกษา	จุฬาลงกรณ์มหาวิทยาลัย	นักศึกษาปริญญาโท	จบการศึกษา
19) นายพชรี สุดาวิชา	นักศึกษา	จบการศึกษา	จุฬาลงกรณ์มหาวิทยาลัย	นักศึกษาปริญญาโท	จบการศึกษา
20) นายวุฒิพงศ์ พงศ์จตุรวิทย์	นักศึกษา	จบการศึกษา	จุฬาลงกรณ์มหาวิทยาลัย	นักศึกษาปริญญาโท	จบการศึกษา
21) นายวิสุทธิ์ วชิรบัญชร	นักศึกษา	จบการศึกษา	จุฬาลงกรณ์มหาวิทยาลัย	นักศึกษาปริญญาโท	จบการศึกษา
22) นายอนวัช ประวาลพิทย์	นักศึกษา	จบการศึกษา	จุฬาลงกรณ์มหาวิทยาลัย	นักศึกษาปริญญาโท	จบการศึกษา
23) นายประธาน วงศ์ศรีเวช	นักศึกษา	จบการศึกษา	จุฬาลงกรณ์มหาวิทยาลัย	นักศึกษาปริญญาโท	จบการศึกษา
24) น.ส.รัตนมณี พาณิชศักดิ์	นักศึกษา	จบการศึกษา	จุฬาลงกรณ์มหาวิทยาลัย	นักศึกษาปริญญาโท	จบการศึกษา
25) น.ส.นงลักษณ์ ชินชุนากร	นักศึกษา	จบการศึกษา	จุฬาลงกรณ์มหาวิทยาลัย	นักศึกษาปริญญาโท	จบการศึกษา
26) น.ส.ชนัญชิดา บุญกระพือ	นักศึกษา	จบการศึกษา	จุฬาลงกรณ์มหาวิทยาลัย	นักศึกษาปริญญาโท	จบการศึกษา
27) น.ส.รัชฎา รัตนมุง	นักศึกษา	จบการศึกษา	จุฬาลงกรณ์มหาวิทยาลัย	นักศึกษาปริญญาโท	จบการศึกษา
28) น.ส. สุกุล ครุเสถียร	นักศึกษา	จบการศึกษา	จุฬาลงกรณ์มหาวิทยาลัย	นักศึกษาปริญญาโท	จบการศึกษา
29) นายนิธิ นิกรณ์ปกรณ์	นักศึกษา	จบการศึกษา	จุฬาลงกรณ์มหาวิทยาลัย	นักศึกษาปริญญาโท	จบการศึกษา
30) นายสันติ วัฒนานุสรณ์	นักศึกษา	จบการศึกษา	จุฬาลงกรณ์มหาวิทยาลัย	นักศึกษาปริญญาโท	จบการศึกษา
31) นายไพศาล คงประสานกาล	นักศึกษา	จบการศึกษา	จุฬาลงกรณ์มหาวิทยาลัย	นักศึกษาปริญญาโท	จบการศึกษา
32) นายนพดล อนุจารีอาภา	นักศึกษา	จบการศึกษา	จุฬาลงกรณ์มหาวิทยาลัย	นักศึกษาปริญญาโท	จบการศึกษา
33) น.ส. สิรีพร คชพันธุ์สุนทร	นักศึกษา	จบการศึกษา	จุฬาลงกรณ์มหาวิทยาลัย	นักศึกษาปริญญาโท	จบการศึกษา
34) นายอนุรักษ์ หวานเสนาะ	นักศึกษา	จบการศึกษา	จุฬาลงกรณ์มหาวิทยาลัย	นักศึกษาปริญญาโท	จบการศึกษา

ชื่อ - นามสกุล	ตำแหน่งวิชาการ		ต้นสังกัด	ตำแหน่งในโครงการ	สถานภาพปัจจุบัน
	เมื่อเข้าร่วมโครงการ	ปัจจุบัน			
35) นายพิชาญ ตันติชัยปกรณ์	นักศึกษา	จบการศึกษา	จุฬาลงกรณ์มหาวิทยาลัย	นักศึกษาปริญญาโท	จบการศึกษา
36) นายอิทธิศักดิ์ สมทรานรักษ์	นักศึกษา	จบการศึกษา	จุฬาลงกรณ์มหาวิทยาลัย	นักศึกษาปริญญาโท	จบการศึกษา
37) น.ส. รวีรัตน์ อิสระธรรมนูญ	นักศึกษา	จบการศึกษา	จุฬาลงกรณ์มหาวิทยาลัย	นักศึกษาปริญญาโท	จบการศึกษา
38) น.ส. บงกช งามสม	นักศึกษา	จบการศึกษา	จุฬาลงกรณ์มหาวิทยาลัย	นักศึกษาปริญญาโท	จบการศึกษา
39) น.ส. ทัศนีย์ วัฒนเชาวน์พิสุทธิ์	นักศึกษา	จบการศึกษา	จุฬาลงกรณ์มหาวิทยาลัย	นักศึกษาปริญญาโท	จบการศึกษา
40) น.ส. นันทมาศ ทัศตะวร	นักศึกษา	จบการศึกษา	จุฬาลงกรณ์มหาวิทยาลัย	นักศึกษาปริญญาโท	จบการศึกษา
41) น.ส. พุธพรรณ จรูญรัตน์	นักศึกษา	จบการศึกษา	จุฬาลงกรณ์มหาวิทยาลัย	นักศึกษาปริญญาโท	จบการศึกษา
42) น.ส. ดารณี สีนา	นักศึกษา	จบการศึกษา	จุฬาลงกรณ์มหาวิทยาลัย	นักศึกษาปริญญาโท	จบการศึกษา
43) น.ส.นริศรา สุขสมัย	นักศึกษา	จบการศึกษา	จุฬาลงกรณ์มหาวิทยาลัย	นักศึกษาปริญญาโท	จบการศึกษา
44) นายกษม สัตยาวุฒิพงศ์	นักศึกษา	จบการศึกษา	จุฬาลงกรณ์มหาวิทยาลัย	นักศึกษาปริญญาโท	จบการศึกษา
45) น.ส. สาวิตรี แสงแก้ว	นักศึกษา	จบการศึกษา	จุฬาลงกรณ์มหาวิทยาลัย	นักศึกษาปริญญาโท	จบการศึกษา
46) นายเกรียงไกร มณีอินทร์	นักศึกษา	จบการศึกษา	จุฬาลงกรณ์มหาวิทยาลัย	นักศึกษาปริญญาโท	จบการศึกษา
47) น.ส. กนิษฐา ผจญอริพ่าย	นักศึกษา	จบการศึกษา	จุฬาลงกรณ์มหาวิทยาลัย	นักศึกษาปริญญาโท	จบการศึกษา
48) น.ส. อรจิรา รุ่งอรุณแสงชัย	นักศึกษา	จบการศึกษา	จุฬาลงกรณ์มหาวิทยาลัย	นักศึกษาปริญญาโท	จบการศึกษา
49) น.ส. สมจิตร วงศ์กำชัย	นักศึกษา	จบการศึกษา	จุฬาลงกรณ์มหาวิทยาลัย	นักศึกษาปริญญาโท	จบการศึกษา
50) นายพรเทพ สิทธิศักดิ์	นักศึกษา	จบการศึกษา	จุฬาลงกรณ์มหาวิทยาลัย	นักศึกษาปริญญาโท	จบการศึกษา
51) นายธีรพงศ์ เจษฎ์ปิยะวงศ์	นักศึกษา	จบการศึกษา	จุฬาลงกรณ์มหาวิทยาลัย	นักศึกษาปริญญาโท	จบการศึกษา
52) นายปริญญา พนาพิศาล	นักศึกษา	จบการศึกษา	จุฬาลงกรณ์มหาวิทยาลัย	นักศึกษาปริญญาโท	จบการศึกษา

ชื่อ - นามสกุล	ตำแหน่งวิชาการ		ต้นสังกัด	ตำแหน่งในโครงการ	สถานภาพปัจจุบัน
	เมื่อเข้าร่วมโครงการ	ปัจจุบัน			
53) นายกิตติศักดิ์ ปึงสมบูรณ์ยิ่ง	นักศึกษา	จบการศึกษา	จุฬาลงกรณ์มหาวิทยาลัย	นักศึกษาปริญญาโท	จบการศึกษา
54) น.ส. ไพริน วิจิตรเจริญเมือง	นักศึกษา	จบการศึกษา	จุฬาลงกรณ์มหาวิทยาลัย	นักศึกษาปริญญาโท	จบการศึกษา
55) นายเมธี ขลไมตรี	นักศึกษา	จบการศึกษา	จุฬาลงกรณ์มหาวิทยาลัย	นักศึกษาปริญญาโท	จบการศึกษา
56) นายณัฐ งามเจตนรมย์	นักศึกษา	จบการศึกษา	จุฬาลงกรณ์มหาวิทยาลัย	นักศึกษาปริญญาโท	จบการศึกษา
57) นายสหัส ไชยโย	นักศึกษา	จบการศึกษา	จุฬาลงกรณ์มหาวิทยาลัย	นักศึกษาปริญญาตรี	จบการศึกษา
58) น.ส.วิไลลักษณ์ ศิริวงศ์รังสรรค์	นักศึกษา	จบการศึกษา	จุฬาลงกรณ์มหาวิทยาลัย	นักศึกษาปริญญาตรี	จบการศึกษา
59) น.ส. ปภาวัลย์ สุทธิประสิทธิ์	นักศึกษา	จบการศึกษา	จุฬาลงกรณ์มหาวิทยาลัย	นักศึกษาปริญญาตรี	จบการศึกษา
60) น.ส. ศิดิภา พงศ์เพรวพรรณ	นักศึกษา	จบการศึกษา	จุฬาลงกรณ์มหาวิทยาลัย	นักศึกษาปริญญาตรี	จบการศึกษา
61) น.ส. บุษรี เมืองถ้ำ	นักศึกษา	จบการศึกษา	จุฬาลงกรณ์มหาวิทยาลัย	นักศึกษาปริญญาตรี	จบการศึกษา
62) นายสุทัศน์ ไหลอุดมสิน	นักศึกษา	จบการศึกษา	จุฬาลงกรณ์มหาวิทยาลัย	นักศึกษาปริญญาตรี	จบการศึกษา
63) นายธีรศักดิ์ เสรีรักษ์	นักศึกษา	จบการศึกษา	จุฬาลงกรณ์มหาวิทยาลัย	นักศึกษาปริญญาตรี	จบการศึกษา
64) นายสานิต ศิริกลการ	นักศึกษา	จบการศึกษา	จุฬาลงกรณ์มหาวิทยาลัย	นักศึกษาปริญญาตรี	จบการศึกษา
65) น.ส. ธัญญรส ภูริปรัชญา	นักศึกษา	จบการศึกษา	จุฬาลงกรณ์มหาวิทยาลัย	นักศึกษาปริญญาตรี	จบการศึกษา
66) น.ส. เอื้อพร นพมงคล	นักศึกษา	จบการศึกษา	จุฬาลงกรณ์มหาวิทยาลัย	นักศึกษาปริญญาตรี	จบการศึกษา
67) นายชนินทร์ วงษ์คนตรี	นักศึกษา	จบการศึกษา	จุฬาลงกรณ์มหาวิทยาลัย	นักศึกษาปริญญาตรี	จบการศึกษา
68) นายประวิทย์ สุรณาภรณ์ชัย	นักศึกษา	จบการศึกษา	จุฬาลงกรณ์มหาวิทยาลัย	นักศึกษาปริญญาตรี	จบการศึกษา
69) นายชล้นวุฒิ นุตยกุล	นักศึกษา	จบการศึกษา	จุฬาลงกรณ์มหาวิทยาลัย	นักศึกษาปริญญาตรี	จบการศึกษา

ชื่อ - นามสกุล	ตำแหน่งวิชาการ		สังกัด	ตำแหน่งในโครงการ	สถานภาพปัจจุบัน
	เมื่อเข้าร่วมโครงการ	ปัจจุบัน			
70) นายพศิ ศรีวสุทธา	นักศึกษา	จบการศึกษา	จุฬาลงกรณ์มหาวิทยาลัย	นักศึกษาปริญญาตรี	จบการศึกษา
71) นายวีรวิทย์ คลังบุญเสริม	นักศึกษา	จบการศึกษา	จุฬาลงกรณ์มหาวิทยาลัย	นักศึกษาปริญญาตรี	จบการศึกษา
72) นายธนโรจน์ ทิมอุดม	นักศึกษา	จบการศึกษา	จุฬาลงกรณ์มหาวิทยาลัย	นักศึกษาปริญญาตรี	จบการศึกษา